11-7-2023

A Bayesian Network-Based Methodology for Improved Bridge Load Rating and Asset Management

Jeffery Mark Roberts
Portland State University

A Bayesian Network-Based Methodology for Improved Bridge Load Rating and Asset Management

by

Jeffery Mark Roberts

A dissertation submitted in partial fulfillment of the
requirements for the degree of

Doctor of Philosophy
in
Civil and Environmental Engineering

Dissertation Committee:
Thomas Schumacher, Chair
Franz Rad
Antonie Jetter
Matthew Smith

Portland State University
2023

Abstract

From the day a new structure is made available for use, to the day that the structure is no longer able to fulfill an intended purpose, structural safety is a vital interest. Managing a portfolio of structures can be a difficult undertaking for an asset manager, particularly if different types of structures are being maintained. The goal is to manage assets in the most efficient manner which can be influenced by, at a minimum, safety and financial concerns.

A potential tool for an asset manager or owner is the use of Bayesian Networks (BNs). When a BN is used to model the structural capacity of individual components and the external loads applied to those components, then an important piece of information becomes available. Through the BN, an asset manager can have an estimate of the component Probability of Failure (P_f). These component values for P_f can be compared directly, or combined to develop estimates of system probabilities of failure. For a bridge portfolio, the asset manager can compare the P_f values of individual girders on a given bridge, or the P_f values of bridges considered as systems of individual components. From these values, the owner can decide how maintenance and replacement activities can be scheduled, where the elements/systems with the higher P_f would be given priority.

The objective of this research is to develop tools that show the viability of using Bayesian Networks to model bridge structures so that an objective estimate of P_f is provided for individual components. To do this, models are created that directly calculate the component capacity (R) taking into account statistical uncertainty of primary variables such as steel yield strength (f_y) and concrete compressive strength (f'_c), in addition to the effects of concrete deterioration. The structural capacity (R) is compared directly to modeled load effects (Q), resulting in a limit state node ($R - Q$), from which the P_f and reliability index, β, are directly determined.

Bridge load ratings are used to indicate how much capacity is present in excess of that needed to support dead loads, or how much live load can still be supported without failure. A load rating can be calculated to reflect a target structural reliability. For example, the AASHTO Load and Resistance Rating (LRFR) load rating process strives for a reliability index of $\beta = 3.5$ for an *Inventory* rating, and a reliability index of $\beta = 2.5$ for an *Operating* rating. A very handy advantage of using BNs to determine the structural P_f and reliability is that the live load can be easily scaled to result in a target reliability, resulting in the direct determination of the load rating factor of the component.

Multiple BNs are described in this dissertation, where bridges using three types of materials are modeled: steel, reinforced concrete, and prestressed concrete. A common thread through each of the examples is to illustrate how the capacities are modeled for each bridge type, how the P_f values are determined, and then how the Rating Factor (RF) values are determined.

An additional strength of using BNs is the ability of the network to be extended. For example, only concrete deterioration is currently considered, but other modes of deterioration could be added to the models to include cross section loss of steel due to corrosion in steel girders or steel reinforcement in concrete members.

This dissertation uses the multi-paper format in accordance with PSU Graduate School guidelines. Therefore, Chapter 1 serves as an introduction, Chapters 2-4 are journal papers that have been published or are under review at the time of dissertation submission, and Chapter 5 is the final chapter with a summary and discussion about future work.

To my partner, Frances,

for her love, support, and friendly ear

Acknowledgments

I would like to express gratitude to my dissertation advisor, Dr. Thomas Schumacher. He has helped me move this work along and has been helpful, inspiring, and motivating during the entire process. The support has been both technical and personal, and greatly appreciated.

Individual supervisors and colleagues at the two U.S. Army Corps of Engineers (USACE) districts that I have worked at have been very supportive of my efforts. These include Bryan Thompson, Michelle Lay, David Jarvis, and Kadiri Venkatesha at the Tulsa district and Erica Tarbox and Matt Hanson at the Portland district.

USACE also supported my attendance at a 6-month temporary duty assignment at the Engineering Research and Development Center (ERDC) located at Vicksburg, MS. Through this assignment, I met Dr. Matt Smith, who supported the research described in this document, and also Dr. Edgardo Ruiz, with whom I worked closely while at ERDC. Equally appreciated was the collaboration with the other ERDC coauthors: Andrew Groeneveld, Dr. Stephanie Wood, and Ricardo Pérez-Gracia. Without the involvement and support of the Corps and ERDC, this research would not have been possible.

I would like to give thanks to Drs. Rad, Jetter, and Smith who served on my dissertation committee. Being a part of this type of work is time consuming and their efforts are greatly appreciated.

Finally, I give thanks to my partner, Frances Lynch, to whom this dissertation is dedicated, and who provided support, encouragement, and helped me be socialized and rational during this experience.

Table of Contents

List of Tables

List of Figures

List of Abbreviations

AASHTO	American Association of State Highway and Transportation Officers
BN	Bayesian Network
CS	Condition State from bridge inspection
DL	Dead Load
DOT	Department of Transportation
COV	Coefficient of Variation (σ/μ)
CPT	Conditional Probability Table used in BNs
ERDC	USACE Engineering and Research Development Center
FHWA	Federal Highway Administration
FOSM	First Order Second Moment
LRFD	AASHTO Load and Resistance Factor Design
LL	Live Load
LR	Load Rating
LRFR	AASHTO Load and Resistance Factor Rating
MBEI	AASHTO Manual for Bridge Element Inspection
NBIS	National Bridge Inspection Standards (23 CFR 650 Subpart C)
NDT	Non-destructive Testing
RF	Rating Factor
SHM	Structural Health Monitoring
USACE	U.S. Army Corps of Engineers

List of Symbols

a	Depth of the equivalent compression block
b_{eff}	Effective flange width of beam
d	Distance from extreme compression fiber to reinforcing steel controid
f'_c	Nominal oncrete compressive strength
f_y	Nominal yield strength
$g()$	Limit state function node in BNs
$M_{Q_{DL}}, M_{Q_{LL}}$	Dead and live moment load effect nodes in BNs
$N(\mu, \sigma^2)$	Normal distribution with specified mean and variance
P_f	Probability of failure
$V_{Q_{DL}}, V_{Q_{LL}}$	Dead and live shear load effect nodes in BNs
β_{calc}	Reliability index ($\beta = \mu_g/\sigma_g$)
β_{P_f}	Reliability index ($\beta = -\Phi^{-1}(P_f)$)
λ	Distribution bias ($\lambda = \mu/nominal$)
μ	General distribution mean
μ_g	Limit state function node distribution mean
σ	General distribution standard deviation
σ_g	Limit state function node distribution standard deviation
$\Phi()$	Standard normal cumulative distribution function

1 Chapter One: Introduction

1.1 Background

From the 2022 National Bridge Inventory (NBI) data, there are over 620,000 bridges with spans greater than 6.10 meters (20 ft) in use in the United States (FHWA 2022). There are various types of materials used with the bridges in the current inventory, but the most common type currently in-service is reinforced concrete, at almost 42%. This includes both simply supported and continuous spans. The next most common materials used are steel and prestressed concrete, at 27.8% and 27.2%, respectively. Timber bridges are still present in the bridge inventory at about 2.5%. Since bridge deterioration is an ongoing concern, bridge owners are required to perform periodic inspections per the Code of Federal Regulations (23 CFR 650 Subpart C). Because the inspection process has some subjective facets, the findings can vary greatly between individuals, teams, and even when a given team inspects a bridge multiple times (Campbell et al. 2019, Moore et al. 2001).

This research uses Bayesian Networks (BNs) to determine the structural reliability, and the Probability of Failure (P_f), of structural components designed using either concrete (reinforced or prestressed) or steel. Extensions of the BNs were developed which allow the structural reliability and P_f to be updated as a result of inspection findings (defects). This is facilitated by linking deterioration mechanisms and findings through expert elicitation (Groeneveld et al. 2021, Roberts et al. 2023) resulting in a reduced concrete compressive strength and reduced flexural and shear capacity, and then ultimately to an increased P_f. Only concrete deterioration is currently considered, but other modes of deterioration could be added to the models to include cross section loss of steel due to corrosion in steel girders or steel reinforcement in concrete members.

Various example structures of the three material types are used to illustrate using BNs to determine the structural reliability and P_f of the structures. The live loads applied to the components are also scaled in order to directly determine rating factors that correspond to target reliability indexes.

The following sections provide an overall view of the modeling methodology with many more details provided in the later chapters.

1.2 Bridge Inspections

Bridge owners are required to perform periodic inspections where the bridge inspection process typically involves, at a minimum, visually assessing the condition of the primary components of a bridge including the deck, railing, superstructure, bearings, and substructure. Each of these components can be broken down further into elements. For example, the superstructure of a girder bridge can be thought of as a collection of girders/beams, stringers and floorbeams. Similarly, the superstructure of a truss bridge can be broken down into truss and gusset plate elements. Each of the individual elements are inspected and assigned condition states, defined in Table 1.1.

Examples of concrete elements in CS3-4 are shown in Fig 1.1. Then, using the condition states of individual elements as a guide, NBI ratings of the bridge components are determined, as defined in Table 1.2. For the purposes of this dissertation, the condition states of the elements are used to account for material deterioration and reduced element/component capacity.

1.3 Bayesian Networks

The structural capacity of each of the components considered was modeled using basic structural mechanics. Fundamental material properties (e.g. reinforcement yield

(a) Delamination (CS4)

(b) Efflorescence (CS3)

(c) Cracking (CS3)

(d) Exposed reinforcement (CS4)

Figure 1.1: Example reinforced concrete defects with condition states (CS) (from USACE 2019).

Table 1.1: Element condition state descriptions (from USACE 2019).

Condition State	Description
1	Any deficiency is minor and has no impact on the performance of the element
2	The deficiency has advanced but with no impact on the performance of the element
3	The deficiency has advanced further and any additional deterioration will impact the strength and/or serviceability of the element
4	The deficiency has advanced to the point where the strength or serviceability of the element may be affected and a structural review is necessary to determine the effect on strength or serviceability of the element or the bridge

strength and concrete compressive strength) are modeled in the BNs as individual parent nodes with appropriate statistical parameters being used (nominal values, coefficient of variation (COV) and bias). These parent nodes are then connected to nodes that represent the capacity of the component. These nodes, that use information from the parent nodes, are known as child nodes. The final child node in the model is the limit state node (gM) that directly provides the P_f of the component. Chapters 2-4 provide more detailed information into the theory and uses of BNs.

1.4 Reliability

The concept of structural reliability is an integral part of this research. As shown in Fig. 1.2, both the resistance (R) and load effect (Q) distributions are used to determine the limit state function ($g = R - Q$). The tail that is located to the left of the $g = 0$ line is where failure occurs, and the P_f value is equivalent to the area under this tail. The reliability index, β, is used to measure how reliable the system/component is by measuring the "distance" the mean (μ_g) of the limit state function is from the onset of

Table 1.2: NBI bridge condition rating descriptions (from USACE 2019 and adapted from FHWA 1995).

NBI Rating		Description
9	Good	EXCELLENT CONDITION
8		VERY GOOD CONDITION - no problems noted
7		GOOD CONDITION - some minor problems
6	Fair	SATISFACTORY CONDITION - structural elements show some minor deterioration
5		FAIR CONDITION - all primary structural elements are sound but may have minor section loss, cracking, spalling, or scour
4	Poor	POOR CONDITION - advanced section loss, deterioration, spalling, or scour
3		SERIOUS CONDITION - loss of section, deterioration, spalling, or scour have seriously affected primary structural components. Local failures are possible. Fatigue cracks in steel or shear cracks in concrete may be present.
2	Severe	CRITICAL CONDITION - advanced deterioration of primary structural structural elements. Fatigue cracks in steel or shear cracks in concrete may be present or scour may have removed substructure support. Unless closely monitored it may be necessary to close the bridge until corrective action is taken.
1		"IMMINENT" FAILURE CONDITION - major deterioration or section loss present in critical structural components, or obvious vertical or horizontal movement affecting structure stability. Bridge is closed to traffic but corrective action may put bridge back in light service.
0		FAILED CONDITION - out of service - beyond corrective action

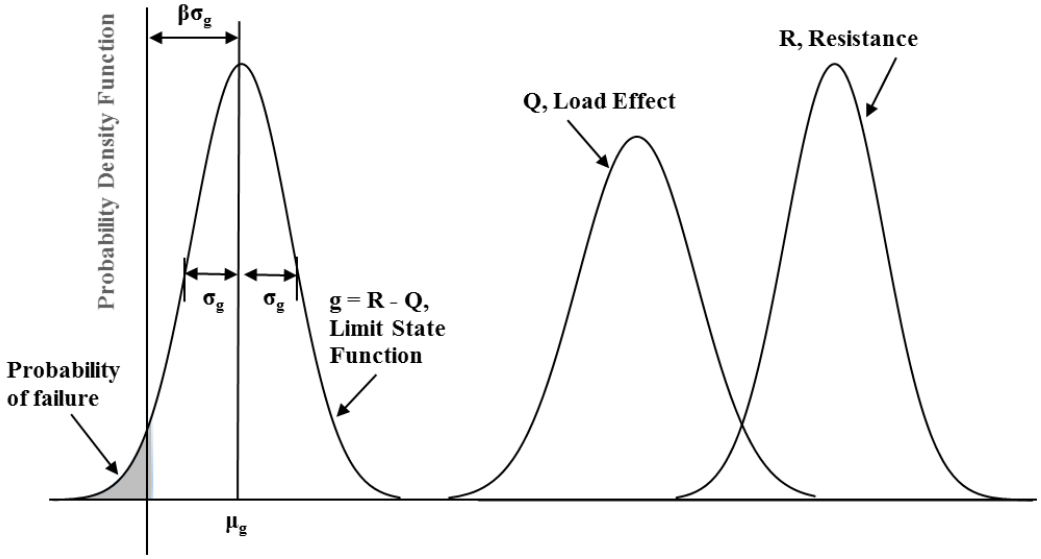

Figure 1.2: Limit state function.

failure ($g = 0$). The reliability index can also be described to be the number of standard deviations the mean is from failure. The larger the reliability index, the more reliable the component/system is said to be. The current AASHTO LRFD design code strives for a reliability index of $\beta = 3.5$ for new structures.

1.5 Load Ratings

Bridge load ratings are used to give a measure of the remaining capacity available from the structure at a specific point in time. Once the dead load is accounted for, the remaining excess capacity available to vehicular design live loads is indicated by the rating factor (RF). If $RF > 1.0$, then the structure is capable of supporting live loads in excess of the minimum design loads. The conventional LRFR equation used to calculate rating factors can be simplified as shown:

$$RF = \frac{\phi_C \phi_S (\phi R_n) - \textit{factored dead loads}}{\textit{factored live loads}} \tag{1.1}$$

where ϕ_C is the component condition resistance factor, ϕ_S is the system resistance factor, and ϕR_n is the factored capacity of the component. The load factors and design live loads are prescribed by AASHTO. The most obvious questions from this equation are regarding how the system and condition factors are determined. The Manual for Bridge Evaluation (AASHTO 2018) provides broad guidance for these values, but the application is very subjective, and can result in a reduction of up to 15% in component capacity.

As part of the required bridge inspections, load ratings are required to be updated to reflect the current condition of the bridge structure. As the bridge ages, the component capacity is likely to decrease, resulting in a reduced rating factor. When sufficient rehabilitation is performed, the rating factor may increase because of improved capacity.

1.6 Material Deterioration

As a result of scheduled bridge inspections, defects of various degrees of severity can be identified. Using current inspection guidelines (AASHTO 2013), the severity of defects are identified as condition states (CS), and vary from least (CS1), to most severe (CS4). The examples shown in Fig. 1.1 illustrate CS3 and CS4 defects. An inspector will determine the presence/absence and severity of defects and determine the overall condition of the elements, components, and bridge. This is part of the subjective nature of the inspection process since bridge components will ultimately be described as being, for example, in a "fair" or "good" state.

Information useful for implementation within BNs could also be provided from in-situ non-destructive testing (NDT) methods including the use of ground penetrating radar (GPR) combined with eddy current testing to estimate the location and diameter of steel reinforcing bars and prestressing tendons, ultrasonic testing to estimate the thickness of structural elements and detect internal voids, and electro-chemical measurements to

estimate the corrosion potential of the reinforcement (ACI 2013).

Recent examples of work that successfully employed NDT information for improved conventional bridge ratings include Bertola et al. 2022 and Küttenbaum et al. 2021. Bertola et al. 2022, in addition to using NDT, used structural health monitoring (SHM) to measure in-service strains for fatigue evaluation. NDT and SHM tools are extremely useful when as-built drawings are incomplete or missing Karshenas and Naghavi 2020.

1.7 Identified Needs

Discussion has been provided that outlines the process of inspecting a bridge structure, and determining rating factors. Common management practices rely on the subjective interpretation of inspection findings to make maintenance and replacement decisions. Load ratings can be used to help with decision making, but determining a rating factor has subjective elements, such as determining the condition factors of the components being evaluated.

The current LRFR rating process uses resistance factors to account for condition and lack of redundancy in the structural system. This is a very broad-stroke method and can reduce capacity by as much as 15%. A system was implemented using the BNs described in this dissertation that accounts for concrete deterioration modes and various defects that may be detected during a bridge inspection. Also, using the concept of parallel and series components and P_f values for individual components, the P_f for a bridge system was estimated allowing for a better estimate of the system reliability index to be calculated.

Since the structural condition has been represented within the BN, and the BN provides directly the reliability index and P_f, the RF can be estimated directly by scaling the modeled live load such that the target reliability index is the result.

1.8 Outline of Dissertation

This dissertation evaluates the use of BNs when determining the condition of existing structures, and examples are provided using in-service bridges. This dissertation follows the multi-paper format in accordance with PSU Graduate School guidelines and is organized as follows:

Chapter One: Introduction.

Chapter Two: Use of Bayesian Networks for Inferences on Bridge Safety. *Abstract:* As bridges deteriorate, uncertainty regarding their safety arises. Common management practices rely on the subjective interpretation of inspection findings to make inferences on bridge safety. A potential solution to this could be the use of Bayesian Networks (BNs) to establish a framework that would incorporate inspection findings with limit state functions to objectively estimate a probability of failure (P_f) with the purpose of inferring bridge safety. This paper focuses on presenting the potential feasibility of this type of approach by comparing the P_f estimated from BN models to a traditional method of estimating structural reliability, First Order Second Moment (FOSM) method. This is performed by approximating a reliability index (β) for the BN by using the estimated P_f. Comparisons were conducted for three bridge types: reinforced concrete girder, prestressed concrete girder and steel composite girder. Results showed that the estimates of P_f from the BN models yielded similar reliability indices (β_{BN}) to those calculated using the FOSM method (β_{FOSM}). In addition to this, β_{BN} were calculated for load effects at inventory and operating levels in order to compare to their corresponding target reliabilities (i.e., β of 3.5 and 2.5 respectively) with results showing that BN models yielded reasonable approximations.

From the 98th Annual Meeting of the Transportation Research Board (presentation no. 19-04278).

Chapter Three: Estimating Reinforced Concrete Bridge Reliability With Inspection Defects Included Using Bayesian Networks. *Abstract:* As part of the bridge inspection process, inspectors identify defects in the main components of the structural system and assign condition ratings. These condition ratings are somewhat subjective since they are influenced by the experience of the inspector. In the current work, procedures were developed for making inferences on the reliability of reinforced concrete (RC) girders with defects at both the cross section, girder, and bridge system levels. The Bayesian network (BN) tools constructed in this study use simple structural mechanics to model the capacity of girders. By using expert elicitation, defects that can be observed during inspections are associated with underlying deterioration mechanisms. By linking these deterioration mechanisms with changes in mechanical properties, inferences on the reliability of a bridge can be made based on visual observation of defects. Also, the BN can be used to directly determine the rating factor (RF) of individual structural elements. Examples are provided using BNs to evaluate both an existing older RC bridge and a new RC design that is based on contemporary AASHTO LRFD specifications.

This paper was submitted to the Journal of Bridge Engineering on 27 April 2023 and is under review.

Chapter Four: Estimating Prestressed Concrete Bridge Reliability and Rating Factors Using Bayesian Networks with an Application to a Bridge Made Continuous for Live Load. *Abstract:* The bridge inspection process has multiple steps. One obvious element is for inspectors to identify defects in the main components of the structural system and assign condition ratings. These condition ratings are somewhat subjective

since they are influenced by the experience of the inspector. In the current work, processes were developed for making inferences on the reliability of prestressed concrete (PC) girders with defects at the girder component level. The Bayesian network (BN) tools constructed in this study use simple structural mechanics to model the capacity of girders. Expert opinion is used to link defects that can be observed during inspections to underlying deterioration mechanisms. By linking these deterioration mechanisms with changes in mechanical properties, inferences on the reliability of a bridge can be made based on visual observation of defects. The BN can then be used to directly determine the rating factor (RF) of individual structural elements. Examples are provided using BNs to evaluate an existing older PC bridge currently behaving as two simply supported spans. The bridge is modeled using two scenarios with the spans acting as simply supported, and then also with the link block (continuity joint) repaired so that the spans are continuous for live load. The spans are considered simply supported for all dead load.

This paper was submitted to the Practice Periodical on Structural Design and Construction on 28 June 2023 and is under review.

Chapter Five: Summary and Future Work.

1.9 References

American Association of State Highway Officials (AASHTO) (2013). *Manual for Bridge Element Inspection*. AASHTO, Washington, D.C., 1st edition. 2015 interims.

American Association of State Highway Officials (AASHTO) (2018). *Manual for Bridge Evaluation*. AASHTO, Washington, D.C., 3rd edition.

American Concrete Institute (ACI) (2013). *Report on Nondestructive Test Methods for Evaluation of Concrete in Structures - 228.2R*. ACI, Farmington Hills, MI.

Bertola, N., Henriques, G., Schumacher, T., and Brühwiler, E. (2022). "Engineering of existing structures: The need and place for non-destructive evaluation." *International Symposium on Nondestructive Testing in Civil Engineering*, Zurich, Switzerland. (August 16-18, 2022).

Campbell, L., Snyder, L., Whitehead, J., Connor, R., and Lloyd, J. (2019). "Probability of detection study for visual inspection of steel bridges: Volume 2 - full project report." *Joint Transportation Research Program Publication FHWA/IN/JTRP-2019/22*, Indiana Dept. of Transportation.

Federal Highway Administration (FHWA) (1995). *Recording and Coding Guide for the Structure Inventory and Appraisal of the Nation's Bridges*. FHWA, Washington, D.C. FHWA-PD-96-001.

Federal Highway Administration (FHWA) (2022). *National Bridge Inventory*. LTBP InfoBridge: Analytics, Washington, D.C., <https://infobridge.fhwa.dot.gov/BarStackChart> (Feb. 19, 2023).

Groeneveld, A., Wood, S., Ruiz, E., and Roberts, J. (2021). "Estimating bridge reliability by using bayesian networks." *U.S. Army Corps of Engineers Engineer (USACE) Research and Development Center (ERDC)*.

Karshenas, A. and Naghavi, B. (2020). "Investigating available state-of-the-art technology for determining needed information for bridge rating strategies." *Report no.*, Louisiana Department of Transportation and Development.

Küttenbaum, S., Braml, T., Taffe, A., Keßler, S., and Maack, S. (2021). "Reliability assessment of existing structures using results of nondestructive testing." *Structural Concrete*, 22(5), 2895–2915.

Moore, M., Pares, B., Graybeal, B., Rolander, D., Washer, G., and Wiss, J. (2001). "Reliability of visual inspection for highway bridges volume 1." *Report No. FHWA-RD-01-105*, Turner-Fairbank Highway Research Center.

Roberts, J., Schumacher, T., Groeneveld, A., Wood, S., and Ruiz, E. (2023). "Estimating reinforced concrete bridge reliability with inspection defects included using bayesian networks." *Manuscript submitted for publication*.

U.S. Army Corps of Engineers (USACE) (2019). *USACE Bridge Inspection Pocket Manual*. USACE, Washington, D.C.

Chapter Two:

Use of Bayesian Networks for Inferences on Bridge Safety

Roberts, J., Ruiz, E., Groeneveld, A., and Pérez-Gracia, R. (2019). "Use of bayesian networks for inferences on bridge safety." Proceedings of the 98th Annual Meeting of the Transportation Research Board, Washington, DC. (Jan 13-17, 2019). Presentation no. 19-04278.

Jeffery M. Roberts [1], Edgardo Ruiz [2], Andrew B. Groeneveld [3], and Ricardo Pérez-Gracia [4]

The authors confirm contribution to the paper as follows: study conception and design: J.M. Roberts, E. Ruiz; analysis and interpretation of results: J.M. Roberts, E. Ruiz, A.B. Groeneveld, R. Perez-Gracia; draft manuscript preparation: J.M. Roberts, E. Ruiz, A.B. Groeneveld, R. Perez-Gracia. All authors reviewed the results and approved the final version of the manuscript.

[1]U.S. Army Corps of Engineers, Tulsa District, 2488 East 81st Street, Tulsa, OK 74137, Email: jeffery.m.roberts@usace.army.mil

[2]Corresponding Author, U.S. Army Engineer Research and Development Center, Geotechnical and Structures Laboratory, 3909 Halls Ferry Road, Vicksburg, MS 39180, Email: edgardo.ruiz@usace.army.mil

[3]U.S. Army Engineer Research and Development Center, Geotechnical and Structures Laboratory, 3909 Halls Ferry Road, Vicksburg, MS 39180, Email: andrew.b.groeneveld@usace.army.mil

[4]U.S. Army Engineer Research and Development Center, Geotechnical and Structures Laboratory, 3909 Halls Ferry Road, Vicksburg, MS 39180, Email: ricardo.perez-gracia@usace.army.mil

2 Chapter Two: Use of Bayesian Networks for Inferences on Bridge Safety

Jeffery M. Roberts, Edgardo Ruiz, Andrew B. Groeneveld,

and Ricardo Pérez-Gracia

2.1 Abstract

As bridges deteriorate, uncertainty regarding their safety arises. Common management practices rely on the subjective interpretation of inspection findings to make inferences on bridge safety. A potential solution to this could be the use of Bayesian Networks (BNs) to establish a framework that would incorporate inspection findings with limit state functions to objectively estimate a probability of failure (P_f) with the purpose of inferring bridge safety. This paper focuses on presenting the potential feasibility of this type of approach by comparing the P_f estimated from BN models to a traditional method of estimating structural reliability, First Order Second Moment (FOSM) method. This is performed by approximating a reliability index (β) for the BN by using the estimated P_f. Comparisons were conducted for three bridge types: reinforced concrete girder, prestressed concrete girder and steel composite girder. Results showed that the estimates of P_f from the BN models yielded similar reliability indices (β_{BN}) to those calculated using the FOSM method (β_{FOSM}). In addition to this, β_{BN} were calculated for load effects at inventory and operating levels in order to compare to their corresponding target reliabilities (i.e., β of 3.5 and 2.5 respectively) with results showing that BN models yielded reasonable approximations.

2.2 Keywords

Reliability, Bayesian Network, Probabilistic, Uncertainty, Bridges, Failure

2.3 Introduction

By the end of the 2016 calendar year, there were over 614,000 highway bridges in use in the United States (FHWA 2016). The structure types vary widely, from common multi-girder structures with 41% of the inventory, to girder/floorbeam systems and trusses at less than 2% each. Reinforced concrete is the most common material type at about 41% of bridges, and the remaining bridges are predominately built using steel and prestressed concrete at about 29% and 24%, respectively. All of these building materials are susceptible to various deterioration and damage mechanisms and thus require the structures to be periodically inspected.

While conducting bridge inspections, condition ratings are determined for the three primary components of a typical bridge (i.e., deck, superstructure, and substructure). When determining component ratings, the inspection team leader is expected to consider the magnitude of deficiencies and the amount that these reduce component performance. These considerations are influenced greatly by the subjective judgment of the inspection team.

There is a level of uncertainty to the condition assessment that leads to an inability to objectively estimate the probability of failure (P_f) of a structure by considering inspection findings. This suggests improvement is needed to the current bridge management approach used by most bridge owners of subjectively interpreting inspection findings by developing an objective framework that incorporates the uncertainty of these inspection findings. A possible approach to achieve this is through the use of Bayesian

Networks (BNs), which are probabilistic graphical models that could facilitate the incorporation of inspection findings to the estimation of probability of failure by accounting for uncertainty in all associated variables.

This paper discusses a probabilistic methodology using BNs to objectively estimate the P_f of a structure. Multiple examples are presented from which the resulting P_f are used to compare to estimates of reliability using the First Order Second Moment method. This methodology, although being discussed in the context of bridges, could be applied to any structure where the concept of failure can be described in terms of capacity and demand.

2.4 Bayesian Networks

BNs are a tool that take into account a grouping of variables, how these variables are related, and the probabilities of interactions (Heckerman and Wellman 1995) and can be used to represent knowledge with the accompanying uncertainty (Pradhan et al. 1996). A key mathematical principle underlying BNs is Bayes' rule, attributed to Thomas Bayes (c. 1701-1761), a British theologian and mathematician (Stone 2013). The general idea is to start with the probabilities associated with a given variable, at a given time. Then, when new data, x, is presented, for example, by observation or measurement, the previous information (or prior probability) can be updated with this new data in mind. Mathematically, this can be presented as:

$$p(\theta|x) = \frac{p(x|\theta)p(\theta)}{p(x)} \tag{2.1}$$

where:

- $p(\theta)$ is the probability of the hypothesis, θ, before the new data is observed, called

the prior probability,

- $p(\theta|x)$ is usually the unknown quantity, or the probability of the hypothesis, θ, given the new data, x, is known, called the posterior probability,
- $p(x|\theta)$ is the probability of the data given the hypothesis is true; called the likelihood,
- $p(x)$ is the probability of the data being true under any hypothesis, and can be considered a normalizing or scaling factor.

Bayes' rule can be used to build upon prior experience, expressed as the prior probability, and combine it with observed data, expressed as the likelihood, to result in the posterior probability. This concept is referred to as Bayesian inference. Since these are probabilistic concepts, Bayesian inference will not guarantee the correct conclusion. However, the inferences will provide the probabilities of possible outcomes, and from these the most probable outcome can become known.

A general example of a simple BN is shown in Fig. 2.1. The nodes, shown in circles, are the variables in the network. The arrows depict the causal relation between the nodes and are referred to as links or edges. In this example, nodes A, B, and C are parents to the child node, D. The location and number of links represents dependencies that are captured by a conditional probability table (CPT) with all possible combinations. The BN allows for inferences on any variable to be made based on information on all other variables by using Bayes' rule (i.e., equation 2.1).

Wright 1921 applied Bayesian statistics to animal husbandry and crop failure problems as the first modern use of BN concepts. In subsequent years, other researchers solved different types of problems using similar ideas such as causal networks (Cooper 1984), belief networks (Cooper 1990), and influence diagrams (Howard and Matheson

2005). All of these uses overlap in that a graphical model is used to represent probabilistic relationships between variables of interest.

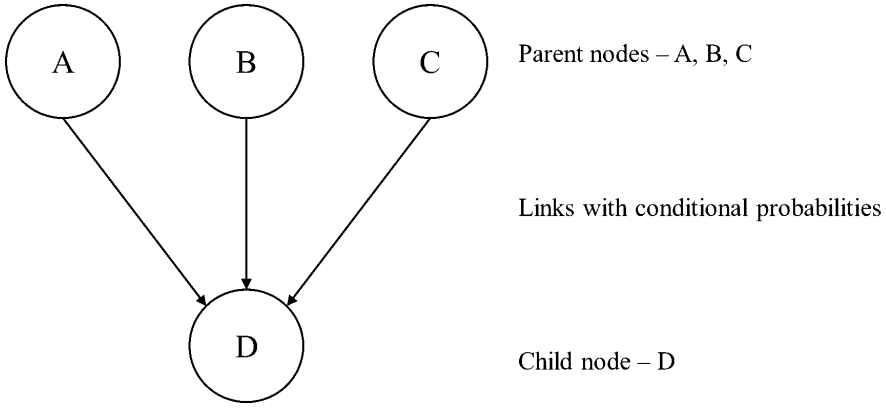

Figure 2.1: Example Bayesian Network.

BNs have been used in various ways ranging from artificial intelligence to mechanical design (Heckerman et al. 1995). More recently, these types of networks have been used to model the various aspects of structures. (Enright and Frangopol 1999) used BNs to predict the deterioration of concrete bridges. Straub and Der Kiureghian 2010a, Straub and Der Kiureghian 2010b, Straub and Papaioannou 2014 have extended the use of BNs to include structural reliability methods. Bateni et al. 2007 have used BNs with a neural network technique to predict scour depth around a bridge pier in addition to the time variation of the depth of scour. BNs have also been used to explore the impact of uncertainty on bridge load rating calculations for a prestressed concrete bridge girder (LeBeau and Wadia-Fascetti 2007, LeBeau 2008, LeBeau and Wadia-Fascetti 2010).

2.5 Structural Reliability

Because of the many components that make up typical structures, an inherently large amount of uncertainty is associated with the related design and construction (Nowak and Collins 2012). Two major categories of uncertainty should be considered: natural

and human. Examples of natural causes include earthquake, wind, snow and ice loads. Human causes encompass all parts of the human condition such as mistakes during the design process, approximations, omissions, or lack of expertise. Since all of the variables associated with a structure, such as individual element dimensions, dead loads and live loads are not exactly, or deterministically, known they should be considered random variables. From an intuitive point of view, we can conclude that with uncertainty, there will always be a probability for the structure to fail since we cannot guarantee that the capacity will always exceed demand. In order to account for uncertainty, codes have evolved to include an acceptable probability of failure, or stated differently, an acceptable reliability.

To be able to determine the reliability of a structure, we must first define what failure means. A simple concept of failure is when the structure fails to perform its designed function. If we can determine, or estimate, the load effect (Q) and the resistance (R), then failure could be defined to be when the resistance is exceeded by the load effect. When $R < Q$, or $R–Q < 0$, then failure occurs. A performance function, or limit state function, $g(R, Q)$, can then be defined as:

$$g(R, Q) = R - Q \tag{2.2}$$

When $g \geq 0$, then the structure is performing its designed function. When g < 0, then the structure has failed. From this, the probability of failure, P_f, can be expressed as:

$$P_f = P(R - Q < 0) = P(g < 0) \tag{2.3}$$

If these variables are assumed to be continuous and random, then P, Q, and g have probability density functions (PDFs) as shown in Fig. 2.2. The area of the limit state

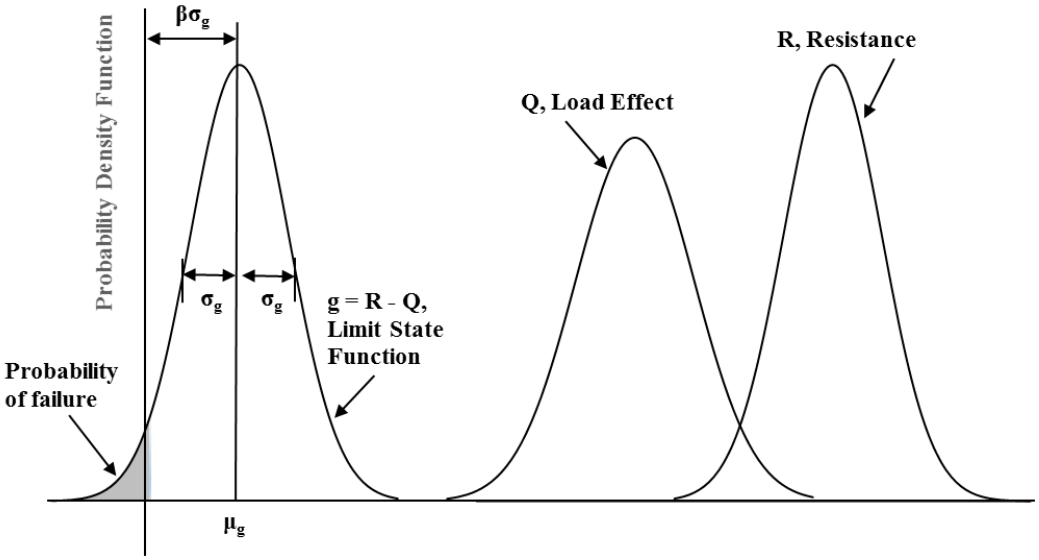

Figure 2.2: PDFs of load, resistance, and limit state function.

curve that is shaded represents the probability of failure, P_f. In contrast, the reliability is the complement of P_f (i.e. $1 - P_f$) or the probability of not failing.

Assuming that g is normally distributed, the reliability index, β, is the ratio of μ_g/σ_g which represents the number of standard deviations that the mean, μ_g, of the limit state function is from a zero value, or the onset of structural failure. If the probability of failure decreases, then the reliability index increases, thus the safety level of the structure increases. Using the equation for β, two possible methods to increase structural reliability would be to increase the mean (μ_g) of the limit state function while maintaining the level of uncertainty (σ_g), or maintain the mean while decreasing the level of uncertainty.

There are numerous methods to find approximations for the reliability index (Nowak and Collins 2012). For example, the First Order Second Moment (FOSM) method provides a closed-form solution assuming a linear limit state function and all variables are uncorrelated. If the variables are also normally distributed, then:

$$P_f = \Phi(-\beta) \tag{2.4}$$

where $\Phi()$ is the standard normal distribution function (zero mean and unit variance) tabulated and found in statistics textbooks. The FOSM method can also be used to obtain an approximate reliability index with non-linear limit state functions by using a Taylor series expansion and only using the linear terms. However, the FOSM method has several shortcomings, one of which is invariance, in that different reliability indices may be found depending on the limit state function chosen. To overcome this, Hasofer and Lind 1974 developed a technique that evaluates the limit state function at a design point instead of using the mean values of the design variables. If the limit state function is nonlinear, then an iterative process is required in order to determine the reliability index.

All of these methods require information on each random variable such as the means and standard deviations, but they do not require information on distribution type. Yet another method was developed by Rackwitz and Flessler 1978 that does require knowledge of the probability distribution type, but can accommodate any type of continuous limit state function and any load distribution type. If desired, a better approximation can be calculated by using the Second Order Reliability Method (SORM). Consistent with the name, the SORM method uses the second order Taylor series expansion as an approximation of the limit state function. However, all of these methods require a well-defined limit state function and can become unwieldy when used with complicated structures. For the work described herein, the FOSM method was used since it was considered to be sufficient for comparison purposes.

2.6 Comparing Bayesian Networks to FOSM Reliability Calculations

Once BNs of a practical size start being used where there are multiple arcs connecting a variety of nodes, the computational complexity increases. This leads to the conclusion

that the only practical way to solve these types of problems is to use numerical software that will account for all of the possible relationships presented in the network to arrive at an approximate solution. For the work presented, Netica version 6.04 (Norsys 2017) was used to develop networks for three different bridge types (i.e., reinforced concrete girder, prestressed concrete girder, and steel girder). Using equation 2.2, the flexural load effect and capacity for each primary load bearing member was defined with the final result being a probability mass function (PMF) for the limit state function. This is then approximated to a PDF as shown in Fig. 2.2. It was assumed that the limit state function was normally distributed. By using equation 2.3, the probability of failure was then determined by calculating the area under the curve where $g < 0$.

In each network, the modeled load effect was based upon the HL-93 live load as defined by the LRFD methodology. It is important to understand that the reliability index that results from a BN (i.e. β_{BN}) is with respect to the live load effect considered. This is in contrast to the LRFR methodology where a load is determined with respect to a target reliability. However, given the parameters used during the development of the BN models are based on those used to calibrate the LRFD factors, if a BN model is built using the same live load effects from which a load rating would result (e.g. $RF_{inventory} \cdot LL$), then it would be expected that the resulting β_{BN} would approximate the target reliability. For this reason, three load effects were considered for each bridge type in order to estimate the reliability index for each case. The first case assumed that the load effect was based solely upon the HL-93 load. The second and third cases were based upon the HL-93 live loads being scaled by the inventory and operating rating factors obtained from load rating calculations. The LRFR load rating calculation (AASHTO 2011), in its simplest form, is:

$$RF = \frac{(\phi C - \gamma_{DL} DL)}{\gamma_{LL} LL} \tag{2.5}$$

where C is the capacity of the member in question, ϕ is an aggregation of resistance factors, γ_{DL} and γ_{LL} are the appropriate load factors for the dead and live loads respectively, and DL and LL represent the dead load and live loads with impact, respectively. This calculation represents the surplus of capacity of a structural member available for the live load once the dead load is accounted for. When the load factors are ignored (i.e., assumed to be unity) such as during modeling within the BN, then the rating factor is a scale that can be applied to the live load. Using these scaled live loads, the corresponding reliability indices can then be determined and compared to the target reliability indices from the LRFD code. The current code assumes that an inventory rating factor corresponds to a target reliability index of 3.5, whereas the operating rating factor corresponds to a reduced target reliability index of 2.5.

2.7 Reinforced Concrete Girder Bridge

A simply supported, 2-girder, 11-span reinforced concrete bridge with maximum span length of 53.5 ft (16.3 m) carrying a county highway located in Oklahoma is used to illustrate the concept of using an FOSM approximation and BN to model structural reliability. The nominal (design) dimensions are shown in Fig. 2.3. The moment carrying capacity of the girder is calculated using:

$$M_n = A f_y \left(d - \frac{a}{2}\right) = A f_y \left(d - 0.59 \frac{A f_y}{f_c' b}\right) = A f_y d - 0.59 \frac{(A f_y)^2}{f_c' b} \tag{2.6}$$

where A is the cross sectional area of the reinforcing steel, f_y is the yield strength of the steel, f_c' is the compressive strength of the concrete, b is the effective width of the girder,

a is the depth of the Whitney rectangular stress distribution, and d is the effective depth of the section.

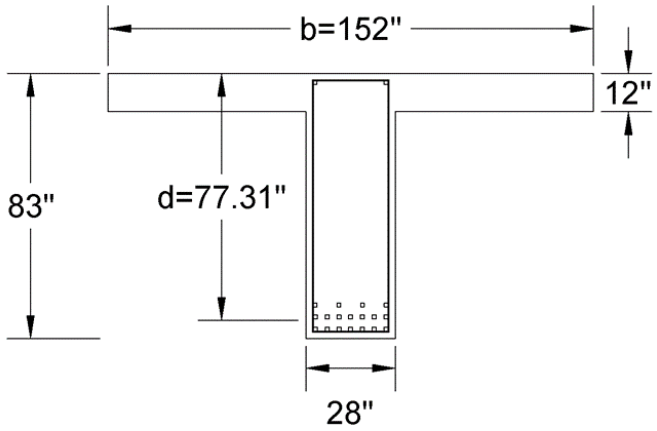

Figure 2.3: Cross section of reinforced concrete girder.

In this analysis, the effective depth and width of the girder are considered deterministic constants. This moment value provides the resistance function, R, required in equation 2.2. The limit state function would then be written as:

$$g = Af_y d - 0.59\frac{(Af_y)^2}{f_c' b} - M_Q \tag{2.7}$$

where M_Q is the moment load effect from all dead loads and HL-93 live loads. The random variables used in the modeling are M_Q, f_y, f_c', and A with the distribution and design parameters provided in Table 2.1.

An estimate of the limit state function for this simple girder can be done using a Taylor series approximation (Nowak and Collins 2012) evaluated at mean values:

$$g\left(X_1, X_2, \ldots, X_n\right) \approx g\left(\mu_{X_1}, \mu_{X_2}, \ldots, \mu_{X_n}\right) + \sum_{i=1}^{n}\left(X_i - \mu_{X_i}\right)\frac{\partial g}{\partial X_i} \tag{2.8}$$

Using this, a general expression for the first-order, second-moment (FOSM) reliability index can then be developed:

Table 2.1: Parameters of random variables.

Material	Parameter	Var.	Units	Nominal	Bias	COV
Reinforced Concrete	Effective width	b	in	152.0	-	-
	Effective depth	d	in	77.31	-	-
	Concrete comp. strength	f'_c	ksi	3.5	1.1	0.18
	Steel yield strength	f_y	ksi	33	1.13	0.12
	Area of reinforcing steel	A	in^2	26.92	1.0	0.015
	Total load effect	M_Q	kips·in	40,200	1.1	0.18
Prestressed Concrete	Width for stress block	b	in	102.0	1.0	0.004
	Effective depth	d_p	in	59.75	1.0	0.011
	Area of prestressing steel	A_{ps}	in^2	4.896	1.012	0.013
	Strand ultimate strength	f_{pu}	ksi	270.0	1.04	0.02
	Concrete comp. strength	f'_c	ksi	4.0	1.10	0.18
	Dead load: cast-in-place	M_{DC}	kips·in	20,640	1.05	0.10
	Dead load: wearing surface	M_{DW}	kips·in	1,944	1.05	0.10
	Live load with impact factor	M_{LL}	kips·in	17,856	1.20	0.18
Steel	Flange thickness	t_f	in	0.855	1.04	0.025
	Web thickness	t_w	in	0.580	1.04	0.025
	Flange width	b_f	in	11.51	0.999	0.002
	Beam height	h	in	33.0	0.999	0.002
	Concrete comp. strength	f'_c	ksi	3.0	1.403	0.10
	Concrete specific weight	w_c	kcf	0.150	1.0	0.03
	Steel modulus of elasticity	E_s	ksi	29,000	1.0	0.06
	Steel yield strength	f_y	ksi	36.0	1.125	0.10
	Live load with impact factor	M_{LL}	kips·in	11,431	1.10	0.18

$$\beta = \frac{g\left(\mu_{X_1}, \mu_{X_2}, \ldots, \mu_{X_n}\right)}{\sqrt{\sum_{i=1}^{n}\left(a_i \sigma_{X_i}\right)^2}} \tag{2.9}$$

where $a_i = \partial g / \partial X_i$ evaluated at the mean values. For our particular problem (with partial derivatives evaluated at mean values), the reliability index is:

$$\beta = \frac{g\left(\mu_{X_1}, \mu_{X_2}, \ldots, \mu_{X_n}\right)}{\sqrt{\left(\sigma_A \frac{\partial g}{\partial A}\right)^2 + \left(\sigma_{f_y} \frac{\partial g}{\partial f_y}\right)^2 + \left(\sigma_{f'_c} \frac{\partial g}{\partial f'_c}\right)^2 + \left(\sigma_Q \frac{\partial g}{\partial Q}\right)^2}} \tag{2.10}$$

Using the values in Table 2.1 to compute the mean (bias·nominal) and standard deviation (COV·mean) and using these with equation 2.10, the FOSM reliability index for the simple reinforced concrete girder can then be estimated to be $\beta = 2.67$.

Next, the same reinforced concrete girder was modeled using Netica with the statistical parameters in Table 2.1. For the BN, all parent nodes were assumed to be normal random variables, with 20 bins being used for all nodes. The network was modified slightly by scaling only the live load using the inventory and operating rating factors. The results for the three cases are provided in Table 2.2. As mentioned earlier, for this work it is assumed that the limit state function is normally distributed. The reliability index from the BN is based on the probability of failure, P_f, which is defined as $P_f = P(g < 0)$. The probability of failure is determined from the output of the BN. The reliability index is then $\beta_{BN} = -\Phi^{-1}(P_{fBN})$, where Φ^{-1} is the inverse of the PDF for the standard normal distribution.

By assuming that the limit state function is normally distributed, the reliability index value, β_{BN}, is calculated. The second reliability index value, β_{FOSM}, represents the reliability index estimate from using the FOSM approximation. The P_{fBN} value is the probability of failure found by summing the area under the limit state function in the BN where $g < 0$.

Table 2.2: Reliability indices result summary.

Material	Case	Applied RF	P_{fBN}	β_{BN}	β_{FOSM}	Difference
Reinforced Concrete	HL-93	1.00	$3.32\text{x}10^{-3}$	2.71	2.67	1.5%
	Inv. RF scaling	0.79	$8.10\text{x}10^{-4}$	3.15	3.09	1.9%
	Opr. RF scaling	1.02	$3.59\text{x}10^{-3}$	2.69	2.63	2.3%
Prestressed Concrete	HL-93	1.00	$6.72\text{x}10^{-11}$	6.42	6.88	-6.7%
	Inv. RF scaling	1.48	$1.87\text{x}10^{-4}$	3.56	3.65	-2.5%
	Opr. RF scaling	1.92	$3.62\text{x}10^{-2}$	1.80	1.78	1.1%
Steel	HL-93	1.00	$1.00\text{x}10^{-3}$	3.09	3.47	-11.0%
	Inv. RF scaling	0.94	$6.41\text{x}10^{-4}$	3.22	3.73	-13.7%
	Opr. RF scaling	1.22	$7.76\text{x}10^{-3}$	2.42	2.57	-5.8%

2.8 Prestressed Concrete Girder

For the prestressed concrete girder example an interior girder in flexure was used. The example bridge is a simply-supported span carrying 2 lanes of traffic. The deck is 8.5 in. (216 mm) thick and is supported by 4 Type IV girders spaced at 8.5 ft (2.60 m). Prestressing steel consists of 0.5 in. (12.7 mm) diameter, 270 ksi (1,860 MPa), low-relaxation strands with a total of 32 strands. Full details on the example structure can be found in AASHTO 2011. To keep the model at a reasonable level of complexity, only the prestressing steel is taken into account for the capacity calculation. The flexural capacity, M_n, can be computed as follows:

$$\beta_1 = \begin{cases} 0.85, & f'_c \leq 4\ ksi \\ 0.85 - 0.05(f'_c - 4\ ksi), & 4\ ksi < f'_c \leq 8\ ksi \\ 0.65, & f'_c > 8\ ksi \end{cases} \tag{2.11}$$

$$c = \frac{A_{ps} f_{pu}}{0.85 f_c' \beta_1 b + k A_{ps} f_{pu} / d_p} \tag{2.12}$$

$$f_{ps} = f_{pu} \left(1 - k \frac{c}{d_p}\right) \tag{2.13}$$

$$a = \beta_1 c \tag{2.14}$$

$$M_n = A_{ps} f_{ps} \left(d_p - \frac{a}{2}\right) \tag{2.15}$$

where f_c' is the 28-day compressive strength of the concrete in the compression zone (deck), A_{ps} is the area of prestressing steel, f_{pu} is the ultimate tensile strength of the prestressing steel, b is the effective flange width, k is a constant (equal to 0.28 for Grade 270 low-relaxation strands), and d_p is the effective depth. Nominal values, bias factors, and coefficients of variation for these variables are given in Table 2.1. The nominal moment due to live load and impact, M_{LL} was 1,488 kip-ft (2,017 kN-m), and a bias factor of 1.2 was selected. The nominal moment due to component dead load, M_{DC}, was 1,720 kip-ft (2,332 kN-m), and that due to wearing surface dead load, M_{DW}, was 162 kip-ft (220 kN-m). A bias factor of 1.05 (cast-in-place) was used for the entire component dead load.

A BN for the flexural capacity limit state was created with the configuration of nodes and edges as shown in Figure 2.4. Netica supports both discrete and continuous variables, the latter of which are discretized into user-specified bins for computation. CPTs may be defined directly; however, it is more convenient to first define the variable with an equation and then use Netica's random sampling to convert the equation into a CPT.

The nodes identified as intermediate variables in Figure 2.4 are defined with equa-

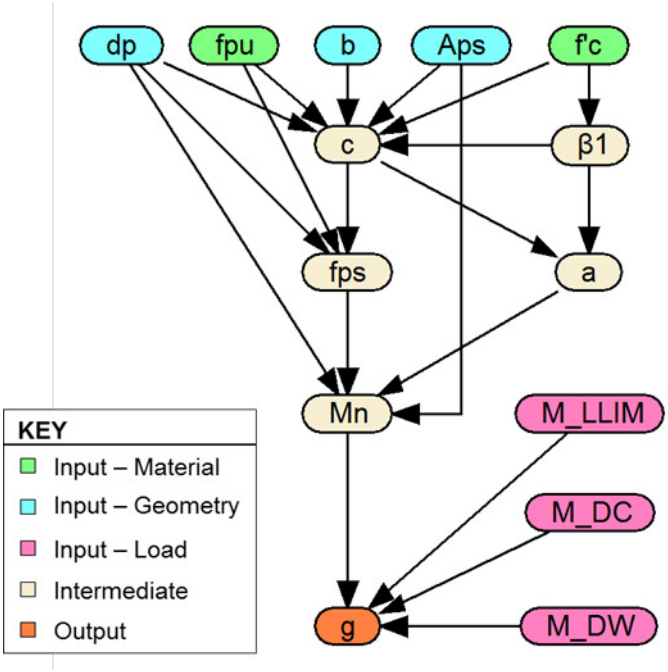

Figure 2.4: Layout of Bayesian network for prestressed concrete girder flexural reliability.

tions 2.11-2.15, and the limit state definition is given by equation 2.2. Input variables were assumed to be normally distributed based on the values found in Table 2.1. It should be noted that BNs are not limited to normally distributed variables. In this work, however, normality was assumed based on a lack of information to support more complex distributions.

The solution of the BN is influenced by the number of bins, n_b, used to discretize each variable and the number of random samples,n_s, taken per cell when generating the CPTs. A brief investigation of convergence was made. The results, shown in Figure 2.5, indicate that there is little change with increasing n_s above 1,000. However, n_b has a strong influence on the results and computation time. The size of the CPTs is driven by the node with the greatest number of parents, in this case c, with 6 parents as seen in Figure 2.4. The size of the CPT for c is $O(n_b^7)$ if all nodes have the same number of bins. Thus, doubling the number of bins entails a 128-fold increase in the size of the

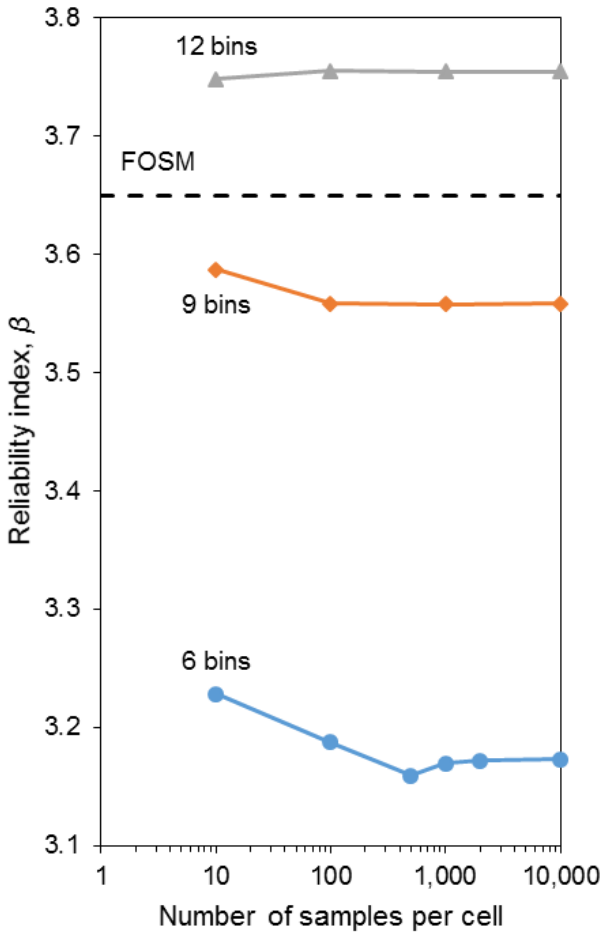

Figure 2.5: Convergence of results with discretization fineness.

CPT for c. Increasing beyond $n_b = 12$ was not feasible with all nodes having the same number of bins. A non-uniform refinement of the discretization could also be used, but this was beyond the scope of the current investigation.

Reliability indices from the BN are given in Table 2.2. As discussed earlier, it is important to consider what load is used to determine the reliability index. If the HL-93 load effects are used, the BN yields a reliability index of 6.42 (probability of failure of 6.72×10^{-11}). The reason for this is that the bridge was designed with excess capacity. A girder with a rating factor of exactly 1 would have exactly the capacity necessary to support the design loads while maintaining the target reliability index. The example

girder has a rating factor of 1.48 (inventory) and 1.92 (operating). Thus, multiplying the load effect by the rating factor should result in approximately the target reliability index. The qualifier approximately is used because the target reliability index is just that—a target. It is approximately satisfied over a range of span lengths, but will not necessarily match for any given individual bridge.

2.9 Steel Girder

The steel example is for a hot-rolled steel girder bridge constructed in 1964. The bridge has a simply-supported span configuration with a maximum span length of 65 ft (19.82 m). Four W33 x 130 beam sections spaced at 7.33 ft (2.23 m) support a concrete deck. The height of a W33 x 130 section is 33.1 in. (84.07 cm), the flange width is 11.51 in. (29.23 cm), the flange thickness is 0.855 in. (2.17 cm) and the web thickness is 0.58 in. (1.47 cm). Lateral stability is provided by C18 x 42.7 channel sections. The girder is a composite section with a concrete deck with a thickness of 7.25 in. (18.41 cm) and a concrete compressive strength of 3 ksi (20.68 MPa). The parameters shown in Table 2.1 were used to compute the mean and standard deviations used in the BN model.

For the computation of the plastic moment capacity, the lateral flexure and buckling failure modes triggered by flexure were not considered since the top flange is continuously restrained by the deck and the plastic neutral axis (PNA) lies within the concrete deck. Therefore the nominal flexure capacity for this example is captured by equation 2.16.

$$M_n = \left(P_w d_w + P_{ft} d_{ft} + P_{fc} d_{fc} + \frac{P_s Y_p^2}{2 t_s} \right) \left[1.07 - 0.7 \frac{Y_p}{h + t_s} \right] \tag{2.16}$$

This expression is based on AASHTO 2017 and is a function of web force (P_w), web force distance (d_w), tension flange force (P_{ft}), tension flange distance (d_{ft}), compression flange force (P_{fc}), compression flange distance (d_{fc}), concrete deck force (P_s), distance

from the top of the concrete deck to the PNA (Y_p), concrete deck thickness (t_s), and beam height (h). All force distances, with the exception of Y_p, are with respect to the PNA.

The load effects for this example included the effect of the HL-93 live load and the dead load for the beam self weight. Notice that in Table 2.1 only parameters for M_{LL} are included. The reason for this is that the M_{DL} was computed within the BN model through the use of the probabilistic distributions already included in the model. The resulting P_f and reliability indices for the steel girder composite section are shown in Table 2.2.

2.10 Summary of results

All of the results are summarized in Table 2.2. The table contains the probability of failure (P_{fBN}) obtained from the BN models, the reliability index (β_{BN}) that was approximated from P_{fBN} and the reliability index (β_{FOSM}) computed using the FOSM method. To verify if the BN models would yield reasonable estimates of probability of failure, the β_{BN} was compared to β_{FOSM}. This was done by computing the percentage difference of β_{BN} with respect to β_{FOSM}. For the most part the differences between these were relatively small (less than 7%). A departure from this was for the steel example where differences were slightly larger (up to 13.7%).

In addition to determining whether the BN model would yield reasonable estimates of probability of failure, they were also gauged against the LRFR target reliability indices by using the live load effects for both inventory and operating levels (3.5 and 2.5, respectively). All β_{BN} cases resulted in values that approximated the target reliabilities.

2.11 Conclusions

A study of the feasibility of BNs for estimating probability of failure was presented in this paper. This was done by comparing estimates of the reliability index of the BN to another more traditional method (i.e., FOSM). The results showed that the BNs yield reasonable estimates of probability of failure since the β_{BN} compared well with β_{FOSM} given the low difference percentages calculated. These difference are suspected to be due to the linearization of a nonlinear function in order to compute the β_{FOSM}. Although the reinforced and prestressed concrete girder examples resulted in very low differences, further investigation should be conducted to determine why there were larger differences in the steel example. The values of β_{BN} estimated also compared well to the target reliability indices to which the load rating factors are calibrated. These results show that the use of BN models would yield comparable results to more traditional methods.

Given the flexibility that BNs have to incorporate uncertainty over traditional methods, these could present an alternative to the subjective nature of inferring the level of safety of a bridge. BNs also have the flexibility to incorporate new variables, such as inspection findings, that would introduce additional layers of uncertainty into an existing model. Although not anticipated to be an easy task, incorporating inspection findings into BN models could result in an objective approach to quantify the level of safety of a bridge by estimating a probability of failure.

BN models do require a computer to perform the required computations. Computational resources are highly dependent on model size (e.g., number of nodes, edges, bins) and therefore must be taken into consideration when developing this type of model. This is especially true for the initial compiling of the model when the CPTs are dependent on the simulations (i.e., relating variables through equations). However these limitations could be overcome by smart modeling or better hardware.

2.12 References

American Association of State Highway Officials (AASHTO) (2011). *Manual for Bridge Evaluation*. AASHTO, Washington, D.C., 2nd edition.

American Association of State Highway Officials (AASHTO) (2017). *LRFD Bridge Design Specifications*. AASHTO, Washington, D.C., 8th edition.

Bateni, S., Jeng, D.-S., and Melville, W. (2007). "Bayesian neural networks for prediction of equilibrium and time-dependent scour depth around bridge piers." *Advances in Engineering Software*, 38(2), 102–111.

Cooper, G. (1984). "NESTOR: A computer-based medical diagnostic aid that integrates causal and probabilistic knowledge." Doctoral dissertation, Stanford University,

Cooper, G. (1990). "The computational complexity of probabilistic inference using bayesian belief networks." *Artificial Intelligence*, 42(2-3), 393–405.

Enright, M. and Frangopol, D. (1999). "Condition prediction of deteriorating concrete bridges using bayesian updating." *Journal of Structural Engineering*, 125(10), 1118–1125.

Federal Highway Administration (FHWA) (2016). *National Bridge Inventory*. Washington, D.C., <https://www.fhwa.dot.gov/bridge/nbi/ascii.cfm?year=2016. Accessed Feb. 10, 2017>.

Hasofer, A. and Lind, N. (1974). "Exact and invariant second-moment code format." *Journal of the Engineering Mechanics Division*, 100(1), 111–121.

Heckerman, D., Mamdani, A., and Wellman, M. (1995). "Real-world applications of bayesian networks." *Communications of the ACM*, 38(3), 24–26.

Heckerman, D. and Wellman, M. (1995). “Bayesian networks.” *Communications of the ACM*, 38(3), 27–30.

Howard, R. and Matheson, J. (2005). “Influence diagrams.” *Decision Analysis*, 2(3), 127–143.

LeBeau, K. (2008). “A bi-directional load rating model of the flexural response of a pre-stressed concrete bridge beam element.” Doctoral dissertation, Northeastern University, Boston, MA.

LeBeau, K. and Wadia-Fascetti, S. (2007). “Comparative probabilistic initial bridge load rating model.” *Journal of Bridge Engineering*, 12(6), 785–793 https://doi.org/10.1061/(ASCE)1084-0702(2007)12:6(785).

LeBeau, K. and Wadia-Fascetti, S. (2010). “Predictive and diagnostic load rating model of a prestressed concrete bridge.” *Journal of Bridge Engineering*, 15(4), 399–407 https://doi.org/10.1061/(ASCE)BE.1943-5592.0000073.

Norsys (2017). *Netica 6.04*. Norsys Software Corp, Vancouver, Canada.

Nowak, A. and Collins, K. (2012). *Reliability of Structures*. CRC Press.

Pradhan, M., Henrion, M., Provan, G., Del Favero, B., and Huang, K. (1996). “The sensitivity of belief networks to imprecise probabilities: an experimental investigation.” *Artificial Intelligence*, 85(1-2), 363–397.

Rackwitz, R. and Flessler, B. (1978). “Structural reliability under combined random load sequences.” *Computers & Structures*, 9(5), 489–494.

Stone, J. (2013). *Bayes’ rule: A tutorial Introduction to bayesian analysis*. Sebtel Press.

Straub, D. and Der Kiureghian, A. (2010a). "Bayesian network enhanced with structural reliability methods: Application." *Journal of Engineering Mechanics*, 136(10), 1259–1270.

Straub, D. and Der Kiureghian, A. (2010b). "Bayesian network enhanced with structural reliability methods: Methodology." *Journal of Engineering Mechanics*, 136(10), 1248–1258.

Straub, D. and Papaioannou, I. (2014). "Bayesian updating with structural reliability methods." *Journal of Engineering Mechanics*, 141(3), 04014134.

Wright, S. (1921). "Correlation and causation." *Journal of agricultural research*, 20(7), 557–585.

Chapter Three:

Estimating Reinforced Concrete Bridge Reliability With Inspection Defects Included Using Bayesian Networks

This paper was submitted to the *Journal of Bridge Engineering* on 27 April 2023 and is under review.

Jeffery M. Roberts[1], Thomas Schumacher[2], Andrew B. Groeneveld[3], Stephanie G. Wood[4], and Edgardo Ruiz[5]

The authors contributed as follows: study conception and design: J.M. Roberts, A.B. Groeneveld, S.G. Wood, E. Ruiz; analysis and interpretation of results: J.M. Roberts, T. Schumacher; draft manuscript preparation: J.M. Roberts, T. Schumacher.

[1]Ph.D. Candidate, Dept. of Civil and Environmental Engineering, Portland State University, Portland, OR 97201. Structural Engineer, U.S. Army Corps of Engineers, Portland District, 333 SW 1st Ave, Portland, OR 97204 (corresponding author). ORCID: https://orcid.org/0000-0002-3505-0580. Email: jeffery.m.roberts@usace.army.mil

[2]Associate Professor, Dept. of Civil and Environmental Engineering, Portland State University, 1930 SW 4th Ave., Portland, OR 97201. ORCID: https://orcid.org/0000-0003-0118-9119. Email: thomas.schumacher@pdx.edu

[3]Research Civil Engineer, U.S. Army Engineer Research and Development Center, Geotechnical and Structures Laboratory, 3909 Halls Ferry Road, Vicksburg, MS 39180, Email: andrew.b.groeneveld@usace.army.mil

[4]Research Civil Engineer, U.S. Army Engineer Research and Development Center, Geotechnical and Structures Laboratory, Vicksburg, MS 39180. Email: stephanie.g.wood@usace.army.mil

[5]Senior Project Manager, Fickett Structural Solutions, Inc., Orlando, FL 32832. ORCID: https://orcid.org/0000-0002-3718-8321. Email: eruiz@fickettinc.com

3 Chapter Three: Estimating Reinforced Concrete Bridge Reliability With Inspection Defects Included Using Bayesian Networks

Jeffery M. Roberts, Thomas Schumacher, Andrew B. Groeneveld,
Stephanie G. Wood, and Edgardo Ruiz

3.1 Abstract

As part of the bridge inspection process, inspectors identify defects in the main components of the structural system and assign condition ratings. These condition ratings are somewhat subjective since they are influenced by the experience of the inspector. In the current work, procedures were developed for making inferences on the reliability of reinforced concrete (RC) girders with defects at both the cross section, girder, and bridge system levels. The Bayesian network (BN) tools constructed in this study use simple structural mechanics to model the capacity of girders. By using expert elicitation, defects that can be observed during inspections are associated with underlying deterioration mechanisms. By linking these deterioration mechanisms with changes in mechanical properties, inferences on the reliability of a bridge can be made based on visual observation of defects. Also, the BN can be used to directly determine the rating factor (RF) of individual structural elements. Examples are provided using BNs to evaluate both an existing older RC bridge and a new RC design that is based on contemporary AASHTO LRFD specifications.

3.2 Introduction

By the end of the 2020 calendar year, there were over 618,000 highway bridges in use in the United States (FHWA 2020). The bridge structure types vary widely, from common multi-girder structures to girder/floorbeam systems and trusses. Reinforced concrete is the most common material type at about 41% of bridges, with steel and prestressed concrete being less common, at about 28% and 26%, respectively. One thing in common among all of these material types is that all of the materials are susceptible to various deterioration and damage mechanisms, possibly leading to bridge component defects. In an attempt to identify relatively small defects prior to developing into significant structural issues, and to improve the long-term performance of bridges, periodic inspections are required by the National Bridge Inspection Standards (NBIS), as found in the Code of Federal Regulations (23 CFR 650 Subpart C). In the current work, defects being considered are as defined in the Manual for Bridge Element Inspection (MBEI) (AASHTO 2013).

Integral to a bridge inspection is the identification of defects and the determination of condition ratings for the three primary components of the typical bridge: deck, superstructure, and substructure. Condition ratings are developed by the inspection team leader by considering the magnitude of deficiencies and the extent that these deficiencies reduce component and system performance. All of these considerations are influenced by the subjective judgement of the inspection team. Therefore, ratings have an element of subjectivity, and ratings for the same structure, even for the same individual components, can vary between different inspection teams and between inspection intervals using the same teams (Campbell et al. 2019, Moore et al. 2001).

There exists a need to quantitatively evaluate inspection findings and to determine the impact on component and system structural reliability. This study develops and

expands the use of Bayesian Networks (BNs) in making inferences on bridge reliability. These inferences are influenced by bridge materials and geometry, but also by observed defects. The illustrated BNs use simple structural mechanics to model the capacity of reinforced concrete girders and expert knowledge is used to link observable defects to deterioration mechanisms that subsequently impact material properties. The end result is that conclusions can be made on structural reliability based upon observable defects.

A load rating analysis was completed in 2016 on a circa 1949 bridge located at a U.S. Army Corps of Engineers (USACE) dam project. Since there has been no observable change in bridge condition, the rating can still be considered valid. The analysis was performed in accordance with then-current design (AASHTO 2014) and rating (AASHTO 2011) guidance. This bridge is used as an example structure to develop several example BNs and to illustrate how the BNs can be used to directly determine rating factors. Additionally, since the BNs can directly provide the probabilities of failure (P_f) of each bridge component, the overall bridge system P_f can then be estimated.

3.3 Bayesian Networks

A BN is a probabilistic graphical model that represents and takes into account a set of variables and how these variable are related and the probability of interaction (Heckerman and Wellman 1995, Pradhan et al. 1996). The BN has the form of a directed acyclic graph (DAG) where nodes represent variables, and edges (links) connect the nodes and represent causal relationships between the variables. A key feature of a DAG is that there are no closed loops within the graph, leading to the acyclic label. The graph is directed because the links represent causality, with links directing the relationship from one or more parent nodes to a child node. The probabilistic nature of the parent/child relationship is captured in conditional probability tables (CPTs). These tables provide the

probability of a child node's state given the state of all parent nodes. A simple network example that is representative of a reinforced concrete beam is shown in Fig. 3.1.

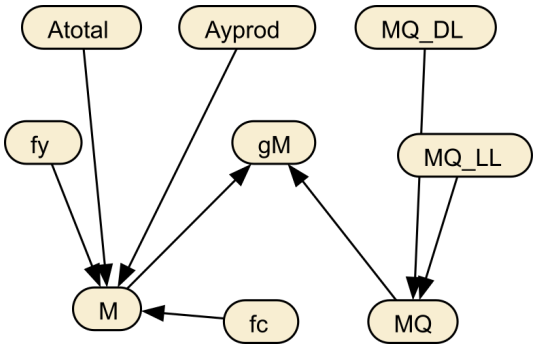

Figure 3.1: Example bayesian network

There are four parent nodes for the moment capacity node (M), and two parent nodes for the total load node (MQ). These two nodes (M and MQ) then act as parent nodes for the limit state node (gM). As will be shown in later sections, the gM node is simply the difference ($gM = M - MQ$) between the parent nodes so that capacity is directly compared to total loads.

3.4 Reliability Analysis

Typical structures are made up of components with inherently a significant amount of uncertainty related to design and construction (Nowak and Collins 2012). While there are multiple categories, two dominant sources of uncertainty to be considered are natural and human. Natural sources can include earthquakes, wind, snow, and ice loads. Human sources can include a wide range of activities such as design mistakes, approximations, omissions, or lack of expertise. Since all the variables associated with physical elements of a structure, such as dimensions and loads, are not exactly known, they can be considered random variables. However, if the variation is relatively small, then some variables can be considered deterministic, from a practical point of view.

With uncertainty, we can always assume that there will be a probability of failure of a component or structure, since we cannot guarantee that capacity will always exceed demand. Some codes have evolved to state a target reliability of the structure, or stated differently, an acceptable probability of failure.

The reliability of a structure is tied closely to the probability of failure of that structure. If the probability of failure is designated as P_f, then we can define reliability to be $1 - P_f$. This means that in order to discuss reliability, then a definition of failure is required. A simple definition of failure could be the structure or component ceases to perform its intended function. Note that this doesn't necessarily require a complete collapse of a structure for failure to occur. Using capacity vs demand, failure can also be defined to mean that demand has exceeded the provided capacity. This can be written in terms of a limit function $g(R, Q)$ defined in terms of two distributions:

$$g(R, Q) = R - Q \tag{3.1}$$

where R represents the structural resistance (capacity) and Q represents the demand (load effect) on the structure. If $g > 0$, then the structural capacity exceeds the demand, and if $g = 0$, then the resistance is exactly equal to the demand. However, when $g < 0$, the resistance is insufficient to support the demand and failure will occur. Graphically, the P_f is the area of the left tail of the limit state function beyond $g = 0$. In terms of the limit state, the probability of failure, P_f, is:

$$P_f = P(g < 0) \tag{3.2}$$

If the Q and R distributions are assumed to be normal, then the limit state function will also be normal, with its own mean and standard deviation. For a limit state function, the reliability index, β, is defined as μ_g/σ_g, where μ_g and σ_g are the mean and standard

deviation, respectively, of $g(R, Q)$. A useful interpretation of the reliability index is that it represents the number of standard deviations that separate the mean value, μ_g, from the initiation of failure ($g = 0$). There are numerous ways to find approximations for the reliability index (Nowak and Collins 2012). The first order, second moment (FOSM) method uses a linear Taylor series expansion of the limit state function, $g(x_1, x_2, ..., x_n)$, about the mean values of its arguments. Assuming the arguments are uncorrelated, the reliability index can be approximated by:

$$\beta_{FOSM} = \frac{g(\mu_{x_1}, \mu_{x_2}, ..., \mu_{x_n})}{\sqrt{\sum_{i=1}^{n} (\sigma_{x_i} \frac{\partial g}{\partial x_i}|_{x=\mu})^2}} \tag{3.3}$$

where the notation $\frac{\partial g}{\partial x_i}|_{x=\mu}$ is used to indicate the evaluation of the partial derivatives at the mean values of each variable.

Another helpful relationship is available if normal distributions are assumed: $P_f = \Phi(-\beta)$, where Φ is the standard normal cumulative distribution function. The inverse is also helpful if the probability is known, and the reliability index is needed: $\beta = -\Phi^{-1}(P_f)$, where Φ^{-1} is the inverse of the standard normal cumulative distribution function.

3.5 Load Rating

The example bridge being used is a two-girder, simply supported, eight-span bridge which carries two lanes of traffic. The superstructure is made of a reinforced concrete deck supported by two reinforced concrete girders where the deck and girders can be considered monolithic. Section and girder elevation drawings are shown in Fig. 3.2. The Load and Resistance Factor Rating (LRFR) methodology (AASHTO 2011) includes both inventory and operating rating factors (RFs). The inventory rating corresponds to

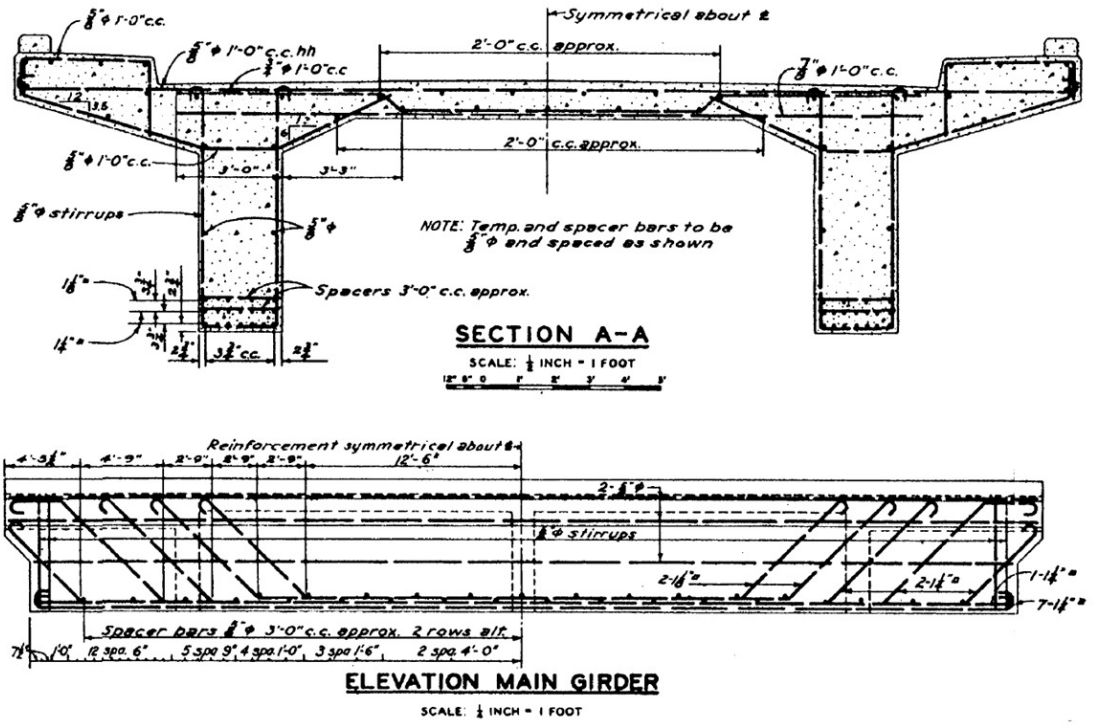

Figure 3.2: Example bridge section and main girder elevation views (reprinted with permission from USACE). Simply supported girders (span of 16.3 m (53.5 ft) c-c bearings and girder spacing of 5.3 m (17.3 ft) c-c bearings).

the magnitude of live load which can safely be supported by a structure for an indefinite amount of time. The LRFD strength limit states (AASHTO 2014) are calibrated to result in an inventory target reliability index of 3.5. The operating RF is comparable to the maximum live loading that may safely be applied to a structure. Allowing an unlimited number of vehicles to use the bridge at this level of loading may decrease the bridge lifespan. The LRFD strength limit states are calibrated to result in an operating target reliability index of 2.5.

For a given component, the LRFR load rating calculation, in its simplest form, is:

$$RF = \frac{\phi_C \phi_S (\phi R_n) - \gamma_{DL} DL}{\gamma_{LL} LL} \tag{3.4}$$

where ϕ_C is the component condition resistance factor, ϕ_S is the system resistance factor, ϕR_n is the factored capacity of the component, γ_{DL} and γ_{LL} represent the appropriate load factors for the dead and live loads, respectively, and DL and LL represent the dead load and live loads. The live load is also calculated using impact and distribution factors. The condition and system resistance factors attempt to reduce the component capacity due to redundancy and condition concerns. In effect, the RF represents the surplus capacity of a structural member available for the live load once the dead load is accounted for. The load (γ_{LL} and γ_{DL}) and resistance (ϕ, ϕ_C, and ϕ_S) factors are not used with BNs since the uncertainties associated with node variables are accounted for directly by using bias and COV values shown in Table 3.1. The bias factor, λ, and COV are defined to be μ/nominal and σ/μ, respectively. The rating factor then acts as a live load scaling factor that can be chosen so that a desired reliability index is the result.

During the most recent load rating performed for the example bridge shown in Fig. 3.2, the design rating factors were determined to be $RF_{inv} = 0.84$ and $RF_{oper} = 1.09$. This rating used HL-93 live loads, and excluded concurrent live loads possible from the under-bridge maintenance catwalk. The girders, from the most recent inspection, were noted to have cracks midspan with efflorescence and spalling. The rating resistance factors were taken to be $\phi_c = 0.95$ and $\phi_s = 0.90$. The flexure condition factor is specified to account for the fair overall superstructure condition and the lowered flexure system factor was used to account for the lack of system redundancy. The product of these two factors is limited (AASHTO 2011) to be no less than 0.85, thus arbitrarily limiting the degree of capacity reduction based on structural condition and lack of redundancy.

LRFR load ratings have a primary advantage in that the calculations are relatively simple, similar to designing using LRFD. However, limitations of LRFR include using the specified, and conservative, HS-20 truck and lack of direct consideration of component redundancy and failure mode correlation Estes and Frangopol 2005. While the current

work makes similar simplifications by using the HS-20 truck, BNs do not preclude the use of different live loads (e.g. through traffic studies accounting for the passage frequency of certain types of trucks), as needed.

3.6 Structural Bayesian Networks

When using the BN to model structural reliability, the limit state function, $g(R, Q)$, is a natural extension of the network. The live and dead load effects are provided directly as inputs with assumed bias and coefficient of variation (COV) values. Likewise, the component capacity is determined using the geometric values and material properties, again with their assumed bias and COV values. The nominal values used in the example BNs, in addition to their statistical attributes, are provided in Table 3.1. Additionally, the same impact and distribution factors used with the conventional load rating was used with the BN.

Using all of the provided values, the BN model can then estimate discretized distributions for the load effects, and also the component moment and shear capacities. All BN development and evaluation were performed using Netica Norsys 2019.

3.6.1 Moment Networks

Roberts et al. 2019 describes the methodology used in this study where structural reliability is modeled using a BN. The example BN presented in Fig. 3.1 represents the network used. For the flexural model (using three layers of longitudinal reinforcement

as shown in Fig. 3.2), the nominal moment capacity is determined using:

$$\begin{aligned} M_n &= f_y A_{S_M} \left(h - \frac{\sum_{i=1}^{3} A_i y_i}{A_{S_M}} - \frac{1}{2} \cdot \frac{f_y A_{S_M}}{0.85 f_c' b_{eff}} \right) \\ &= f_y A_{S_M} \left(d - \frac{a}{2} \right) \end{aligned} \tag{3.5}$$

where f_y is the reinforcing steel yield strength, f_c' is the compressive strength of the concrete, A_{S_M} is the total area of flexural reinforcing steel and $A_i y_i$ provides the area and vertical location of reinforcement for the i^{th} layer, $d = h - (\sum_{i=1}^{3} A_i y_i)/A_{S_M}$ represents the distance from the extreme compression fiber to the reinforcing steel centroid with h being the height of the girder, and $a = (f_y A_{S_M})/(0.85 f_c' b_{eff})$ represents the depth of the equivalent compression block with b_{eff} being the effective flange width of the girder.

Initial BN models for a simple RC beam used nodes for each individual layer of reinforcing steel Roberts et al. 2019. This allowed the model to account for each layer explicitly but unfortunately resulted in relatively large conditional probability tables (CPTs). One approach to minimize the computational impact of having larger CPTs is to use the idea of variable reduction Groeneveld et al. 2021. This approach removes the need to individually account for each reinforcement layer by utilizing a single intermediate node that uses a normal distribution approximation for the product $A_i y_i$. Generally speaking, the product (XY) of two uncorrelated normal distributions, $X \sim N(\mu_X, \sigma_X^2)$ and $Y \sim N(\mu_Y, \sigma_Y^2)$, is the sum of two χ^2 random variables, and approaches the distribution $N(\mu_X \mu_Y, \mu_X^2 \sigma_Y^2 + \mu_Y^2 \sigma_X^2)$ as the inverse coefficient of variations ($\delta_X = \mu_X/\sigma_X$ and $\delta_Y = \mu_Y/\sigma_Y$) increase in magnitude Seijas-Macías and Oliveira 2012. For our purposes, we will assume that inverse coefficients $\delta > 1$ are sufficient. All presented BNs will use this intermediate node which has units of mm^3 (in^3). The attributes used for area, A_i, and location, y_i, will be $A_i \sim N(\mu_{A_i}, \sigma_{A_i}^2)$ and $y_i \sim N(\mu_{y_i}, \sigma_{y_i}^2)$, respectively. Since adding normal distributions results in a new normal distribution, the summation of normally

approximated $A_i y_i$ products can also be approximated as normal.

Most of the remaining BN nodes are constructed assuming normal distributions and using the nominal, bias, and COV values provided in Table 3.1. Mean values are calculated using the bias (μ = bias·nominal), and standard deviations are determined using the COV (σ = COV·μ). The flexural steel area, yield strength, concrete compressive strength, and live and dead load effect nodes are all constructed assuming normal distributions, and discretized into 20 bins with a total width of eight standard deviations ($\mu \pm 4\sigma$). The higher number of bins is necessary to provide a reasonable approximation for the normal distribution and was determined by increasing the degree of discretization until an asymptote was observed for the probability of failure.

The limit state node is the remaining node not yet discussed for the BN. As described previously, the limit state function is defined as $g(R, Q) = R - Q$, with R and Q being the capacity and load, respectively. The limit state node uses this relationship and simply subtracts the total load effect distribution from the moment capacity distribution. All the nodes that make up a simple moment BN are shown in Fig. 3.3. Each node shows the discretization of the distribution with values and probabilities (represented as percentages) associated with each bin. Each node also provides the mean and standard deviation, shown at the bottom of each node. For example, the moment limit state node shows a mean and standard deviation of μ_g=3,434.7 kN·m (30,400 kip·in) and σ_g=1,062.1 kN·m (9,400 kip·in), respectively. The unique information found from the limit state node is the probability of failure of the component represented by the BN. The portion of the limit state function where $g < 0$ (i.e., demand exceeds capacity) provides the probability of failure of the component. In this example, $P_f = 5.57\text{x}10^{-4}$.

The reliability index, β, can also be estimated using two approaches. If we use the definition of reliability index, the value can be directly found: $\beta = \mu_g/\sigma_g$ = 3,434.7 kN·m / 1,062.1 kN·m = 30,400 kip·in / 9,400 kip·in = 3.23, using the values directly

Table 3.1: Parameters of variables used in bayesian networks of two-girder example bridge

Definition of random variables	Notation	Nominal value	Bias $\left(\frac{\mu}{nominal}\right)$	COV $\left(\frac{\sigma}{\mu}\right)$	References[a] for bias/cov
Conc. comp. strength	f'_c	24.13 MPa (3.5 ksi)	1.10	0.18	LE08
Steel yield strength (<1970s)	f_y	227.53 MPa (33.0 ksi)	1.13	0.10	EGMC80
Steel yield strength (>1970s)	f_y	413.69 MPa (60.0 ksi)	1.13	0.02	NRS12
Total flexural area of steel	A_{S_M}	17,367 mm^2 (26.92 in^2)	-	-	-
Top layer	A_3	7,045 mm^2 (10.92 in^2)	1.00	0.015[b]	NYT94
Middle layer	A_2	7,045 mm^2 (10.92 in^2)	1.00	0.015[b]	NYT94
Bottom layer	A_1	3,277 mm^2 (5.08 in^2)	1.00	0.015[b]	NYT94
Centroid total flexural steel[c]	$y_{c.g.}$	From layer distributions	-	-	-
Top layer	y_3	260.35 mm (10.25 in)	1.00	SD[d]	NYT94
Middle layer	y_2	165.1 mm (6.50 in)	1.00	SD[d]	NYT94
Bottom layer	y_1	69.85 mm (2.75 in)	1.00	SD[d]	NYT94
Total shear area of steel	A_{S_V}	396 mm^2 (0.614 in^2)	1.00	0.015	NYT94
Moment load effect - Live[e]	$M_{Q_{LL}}$	1,714.32 kN·m (15,173.0 kip·in)	1.40	0.18	NS00 & NC12
Moment load effect - Dead	$M_{Q_{DL}}$	2,699.30 kN·m (23,890.8 kip·in)	1.05	0.10	NO95 -
Shear load effect - Live[e]	$V_{Q_{LL}}$	254.88 kN (57.3 kip)	1.40	0.18	NS00 & NC12
Shear load effect - Dead	$V_{Q_{DL}}$	198.84 kN (44.7 kip)	1.05	0.10	NO95
Shear constants[f]	β_c, θ	1.52, 32.85°	-	-	-
Effective flange width[g]	b_{eff}	4,572.0 mm (180 in)	-	-	-
Girder height[g]	h	2,133.6 mm (84 in)	-	-	-

[a] LE08:LeBeau 2008; EGMC80:Ellingwood et al. 1980; NRS12:Nowak et al. 2012; NYT94:Nowak et al. 1994; NS00:Nowak and Szerszen 2000; NC12:Nowak and Collins 2012; NO95:Nowak 1995.
[b] Total area is calculated assuming the sum of normal distributions will also be normal. The bias and COV are used for each layer.
[c] Vertical distances to reinforcement centroids are referenced to bottom girder edge.
[d] The error in positioning layer reinforcement does not change based on the depth of the member. Therefore, the variability of the vertical positioning, y_i, of the flexural reinforcement is given in terms of the standard deviation (SD) rather than COV. The bias and a standard deviation of 17.78 mm (0.7 in) are used for each layer.
[e] Live load includes an impact factor of 1.33 and distribution factor of 1.106.
[f] Shear constants were previously determined in accordance with AASHTO 2014 and are considered deterministic.
[g] The effective width and height of the girder are considered deterministic.

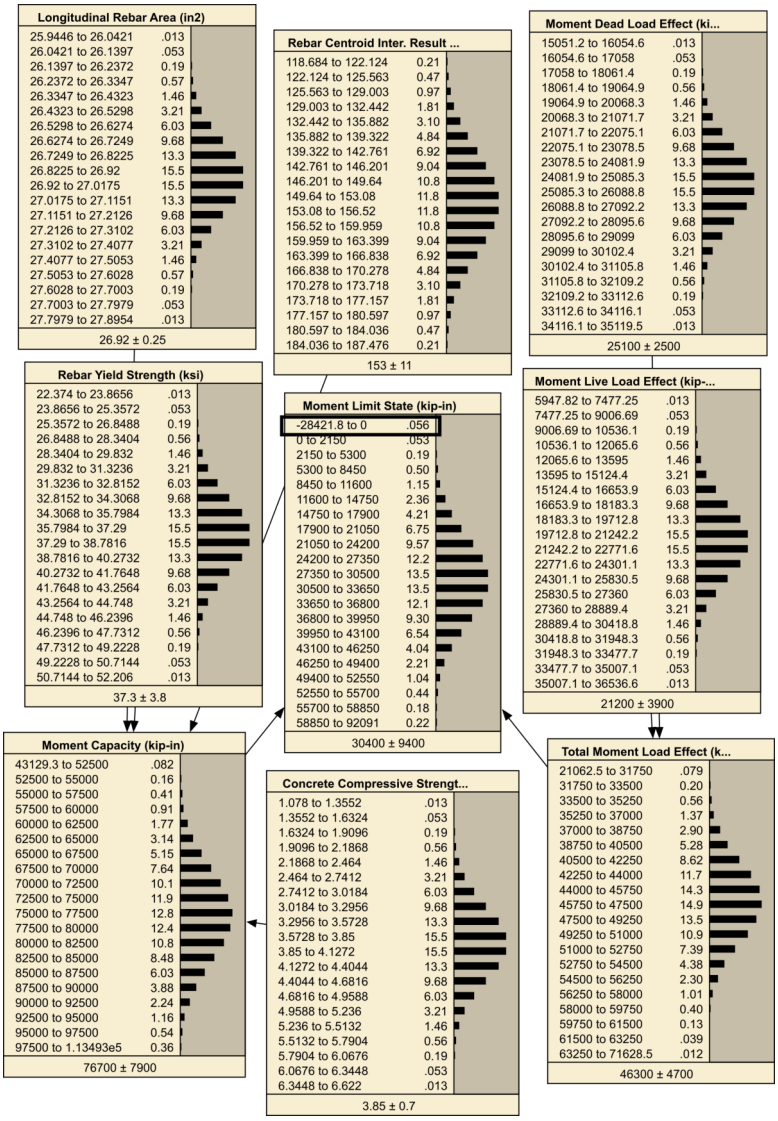

Figure 3.3: Girder moment bayesian network with discretized distributions. Area of moment limit state function where $g(R,Q) < 0$ provides probability of failure, P_f = 5.57x10^{-4}. Moment limit state mean and standard deviation are μ_g = 3,434.7 kN·m (30,400 kip·in) and σ_g = 1,062.1 kN·m (9,400 kip·in), respectively. $\beta_{calc} = \mu_g/\sigma_g$ = 3.23. $\beta_{P_f} = -\Phi^{-1}(5.57x10^{-4}) = 3.26$.

from the limit state node. The second method is to assume the distribution is normal, and use the inverse of the standard normal cumulative distribution function, Φ^{-1}. In this case, $\beta = -\Phi^{-1}(0.000557) = 3.26$. Since all the distributions being used are normal, the expectation is that the reliability indexes found using the two methods should be very

similar. If we revisit the idea of rating factors in the context of structural reliability, these results are consistent with an operating factor exceeding 1.0 since the goal of the operating factor is to provide a reliability index of 2.5. A contrasting viewpoint could be that the reliability index represents an inventory rating factor less than 1.0, since $\beta < 3.5$.

3.6.2 Shear Networks

To assemble the shear BN model, the nominal shear capacity is determined using conventional methods prescribed by AASHTO 2014. The current load rating calculation for the example bridge (Fig. 3.2) uses angled longitudinal bars which can be used to add shear capacity. The current study only addresses shear capacity at the location that was previously determined to be the governing location for shear, which is 5.7 m (18.75 ft) from the bearing centerline. This is somewhat surprising being so distant from the bearings, but the stirrup spacing is relatively large at 1.22 m (4.0 ft) on centers. This wide stirrup spacing, with the HL-93 live load, leads to the governing shear being closer to the girder center. The relations used to determine shear capacity are:

$$V_c = 0.0316\,\beta_c\,\sqrt{f_c'}\,b_v\,d_v \tag{3.6}$$

$$V_s = \frac{A_{S_V}\,f_y\,d_v\cot\theta}{s} \tag{3.7}$$

$$V_n = V_c + V_s \tag{3.8}$$

where θ is the inclination angle of the diagonal compressive stresses in the web, β_c is a factor for tensile stresses in the cracked concrete, f_c' is the concrete compressive strength, b_v and d_v are the girder width and effective depth, respectively, A_{S_V} is the total area of the shear reinforcement, f_y is the yield strength of the reinforcement, and s is the spacing of the shear reinforcement. The total nominal shear capacity, V_n, is the sum of

the capacity due to the concrete itself, V_c, and the contribution from steel reinforcement, V_s. The β_c and θ values, as provided in the LRFD design code, are dependent upon the factored moment (M_U) and shear (V_U) load effects at each location along the length of the girder. For simplification, the current BN will use previously determined β_c and θ values for the location where the minimum shear rating factor occurs, and assume these parameters are deterministic. Angled longitudinal reinforcement can be used to increase shear capacity, if present. However, the assumed location of the governing shear occurs where the longitudinal reinforcement is not angled, therefore Eqns. 3.6 - 3.8 describe the total available shear capacity. The parameters used in the shear BN are provided in Table 3.1.

The shear limit state node uses the limit state function $g(R, Q) = R - Q$, with R and Q being the capacity and load, respectively. All the nodes that make up a simple shear BN are shown in Fig. 3.4. The shear limit state node shows a mean and standard deviation of μ_g = 578.3 kN (130 kip) and σ_g = 120.1 kN (27 kip), respectively. The portion of the limit state function where $g < 0$ (i.e., demand exceeds capacity) provides the probability of failure of the component. For the shear BN, P_f = 9.01x10^{-6}. Although this value is not apparent in the network shown in the figure, the value is available through the Application Programming Interface (API) used in this investigation. The reliability index, β, calculated from the BN is $\beta = \mu_g/\sigma_g$ = 578.3 kN / 120.1 kN = 130 kip / 27 = 4.81 by using the values directly from the limit state node. Using the second method, by assuming a normal distribution, yields $\beta = -\Phi^{-1}(9.01x10^{-6}) = 4.29$. These results are consistent with an inventory rating factor well exceeding 1.0 since the goal of the inventory factor is to provide a reliability index of 3.5.

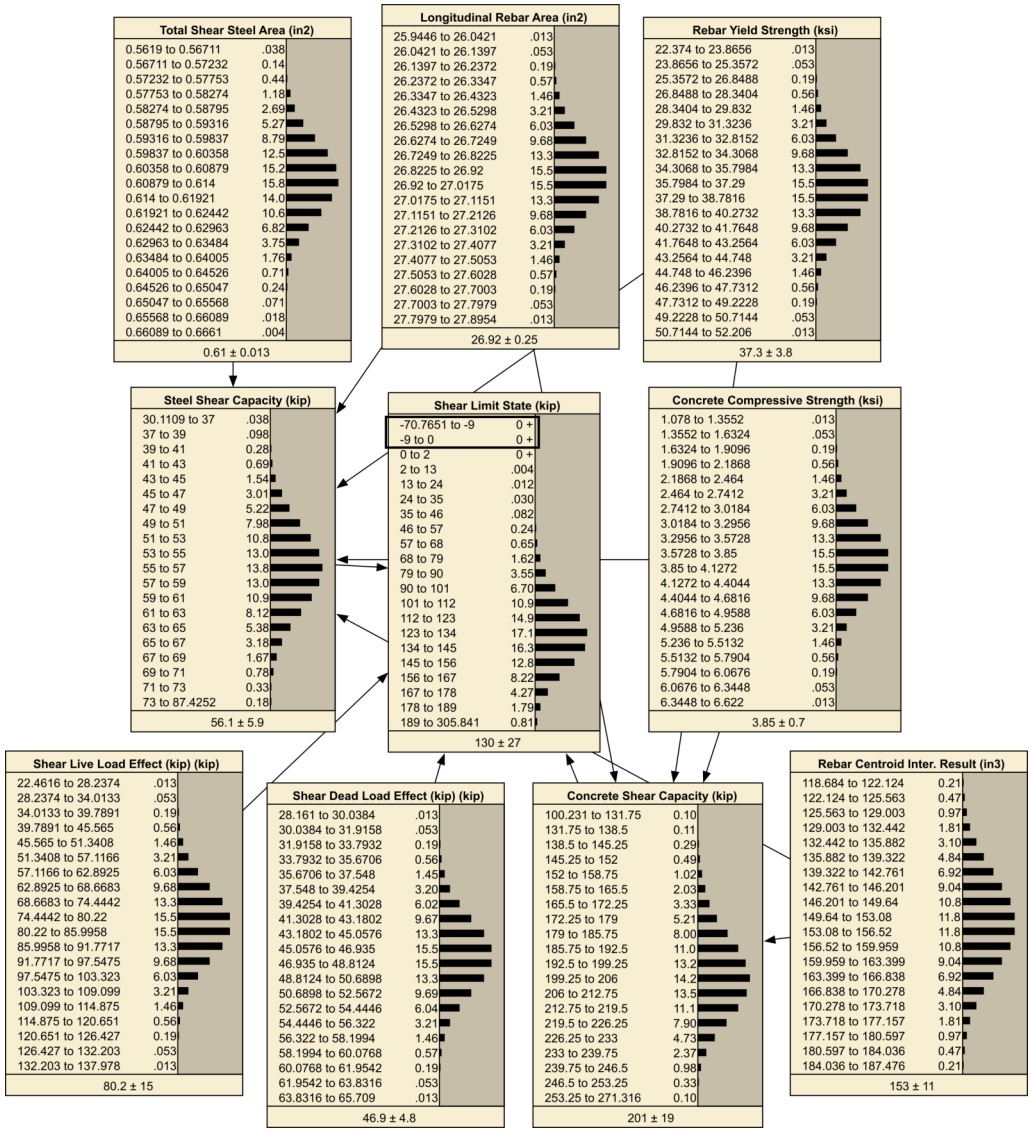

Figure 3.4: Girder shear bayesian network with discretized distributions. Area of shear limit state function where $g(R,Q) < 0$ provides probability of failure, P_f = 9.01x10^{-6}. Shear limit state mean and standard deviation are μ_g = 578.3 kN·m (130 kip) and σ_g = 120.1 kN (27 kip), respectively. $\beta_{calc} = \mu_g/\sigma_g = 4.81$. $\beta_{P_f} = -\Phi^{-1}(9.01x10^{-6}) = 4.29$.

3.7 Material Deterioration

Typical defects found in concrete structures can be caused by either damage to the structure or by deterioration. Sources of damage to a bridge can range from impact or overloading, all possibly due to vehicles such as large ships or trucks. Common deterioration modes for concrete include corrosion of reinforcement, effect of freeze-thaw (FT) cycles, and the alkali-silica reaction (ASR). The current BNs will only include specific effects of several types of deterioration. The types of defects being considered, associated with likely deterioration modes, are shown in Table 3.2. A detailed description of these deterioration modes can be found in Groeneveld et al. 2021.

Table 3.2: Common defects correlated with deterioration modes

Defect	Deterioration mode
Cracking	Corrosion, FT Effect, ASR
Spalling	Corrosion, FT Effect, ASR
Delamination	Corrosion, FT Effect
Efflorescence	FT Effect, ASR
Rust staining	Corrosion
Exposed reinforcement	Corrosion
Pattern cracking	ASR

Beyond considering defects, additional information useful for implementation within BNs could be provided from in-situ non-destructive testing (NDT) methods. Examples include using ground penetrating radar (GPR) combined with eddy current testing to estimate the location and diameter of steel reinforcing bars and prestressing tendons, ultrasonic testing to estimate the thickness of structural elements and detect internal voids, and electro-chemical measurements to estimate the corrosion potential of the reinforcement ACI 2013. Basic material properties, such as the concrete modulus of elasticity and compressive strength, can be determined by either testing cores extracted

from existing structures or in-place also using NDT techniques ACI 2019. As noted in Lequesne and Collins 2020, NDT is still not frequently used due to some of the errors and uncertainties associated with the measurements, which could be accommodated within a BN framework. Some recent examples of work that successfully employed NDT information for improved bridge ratings include Bertola et al. 2022 and Küttenbaum et al. 2021. Bertola et al. 2022, in addition to using NDT, employed structural health monitoring (SHM) to measure in-service strains for fatigue evaluation. NDT and SHM tools become of critical importance when as-built drawings are incomplete or missing Karshenas and Naghavi 2020.

The defects described above, and listed in Table 3.2, are presented as nodes in the BNs so that findings can be reported to the network. For example, inspection findings are shown in Fig. 3.5 at a condition state CS1 level. The severity of each defect is defined consistent with the MBEI AASHTO 2013, and as such, defects range from CS1 (good) to CS4 (severe). All of the nodes have choices available from CS1 to CS4, with the exception of pattern cracking which simply has a yes/no choice to indicate presence/absence of the defect.

In order to connect the defects in Table 3.2 to each mode of deterioration, conditional probability tables (CPTs) were constructed. The CPT provides the probability of a given defect being caused by a specific deterioration mode at varying levels of severity. The values in the CPTs were selected by expert elicitation and should not be considered as precise, but as an estimate of the relative impact of defects on concrete compressive strength. This illustrates the advantage of using BNs to ultimately estimate structural reliability, in that experience and research can improve, over time, the CPTs used in the networks. The CPTs are how our "best estimate" at a given point in time can be expressed. Examples of research linking freeze-thaw cycles with mechanical properties of concrete are provided in Ji et al. 2008, Shang et al. 2014 and Hanjari et al. 2008. BNs

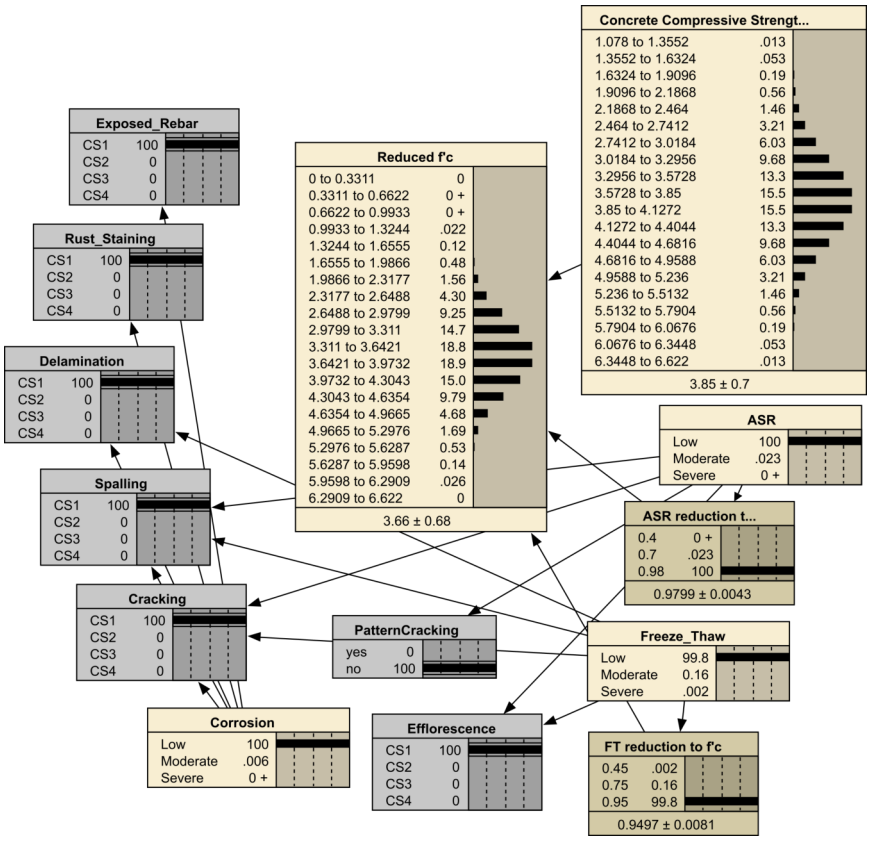

Figure 3.5: Example network with defects assumed at condition state CS1. Defects include: exposed reinforcement, rust staining, delamination, spalling, cracking, pattern cracking, and efflorescence. Initial concrete compressive strength has mean and standard deviation of 26.54 MPa (3.85 ksi) and 4.84 MPa (0.702 ksi), respectively. The *Reduced* f_c' node provides final concrete compressive strength after CS1 defect findings are entered, and has mean and standard deviation of 25.23 MPa (3.66 ksi) and 4.70 MPa (0.681 ksi), respectively.

in the current work include the effects of deterioration on the compressive strength of concrete Groeneveld et al. 2021 where future work will include the effects of section loss of reinforcement due to corrosion.

An example of a CPT for concrete cracking is given in Table 3.3. The provided table shows that cracking is influenced by ASR, FT, and Corrosion. Note also that the provided CPT table is incomplete since only a Low ASR severity is given, whereas Low, Moderate, and Severe levels are shown for the other defects. A full CPT that

Table 3.3: Partial conditional probability table (CPT) for concrete cracking condition states (CS1-4). Only *Low* levels of severity are shown for ASR.

			Cracking CS			
ASR	FT	Corrosion	1	2	3	4
Low	Low	Low	90	5	4	1
Low	Low	Moderate	10	37	38	15
Low	Low	Severe	5	10	15	70
Low	Moderate	Low	15	35	30	20
Low	Moderate	Moderate	8	15	27	50
Low	Moderate	Severe	2	10	13	75
Low	Severe	Low	5	15	30	50
Low	Severe	Moderate	2	8	37	53
Low	Severe	Severe	2	6	32	60

includes the Moderate and Severe levels for ASR would therefore have a total of 27 rows. A complete set of CPTs can be found in Groeneveld et al. 2021. This sample table illustrates the probability of observing a defect given the severity of deterioration. From Fig. 3.6, arrows are directed from ASR to the spalling, cracking, pattern cracking, and efflorescence nodes. This means that ASR can be the cause of these defects. Using Table 3.3, this relationship is quantified. From the first row, when ASR, FT, and Corrosion have low severities, there are 90%, 5%, 4%, and 1% probabilities of cracking being at CS1, CS2, CS3, and CS4 states, respectively. Note that each row must sum to 100% to completely account for all possibilities. The inverse problem can also be addressed, which is probably the most intuitive use of this type of tool. This allows the user to predict possible root causes of observable defects using Bayesian inference. For example, if results from an inspection (refer to Fig. 3.6) are provided to the tool (e.g. spalling at CS3, cracking at CS3, and efflorescence at CS1) then there is a 70.6% probability of the presence of ASR at a low level of severity. However, there is also a 29% probability of ASR at a moderate level and a very low probability (0.39%) of severe ASR.

3.8 Example Bayesian Networks with Inspection Findings

Several case examples of BNs will be used where various defects and defect locations are illustrated. Detailed explanations for each case are provided in the Appendix. Table 3.4 outlines all of the case examples. Cases 1-4 focus on an individual girder, with varying defects. These defects are specified to be either uniform along the entire length of the girder member, concentrated at girder midspan, or of differing severity along the girder with the girder being defined into separate segments. The methodology used to separate a girder into segments is described in the Appendix. Case 5 includes a girder pair, as in the example bridge. The CS3 defects will be assumed to be centered midspan with CS1 conditions elsewhere along the girder. Case 6 will also include a girder pair, but with multiple defects of varying severity along one girder. The overall intent of these cases is to demonstrate the relative ease that different bridge and component conditions can be accommodated when using BNs.

These six cases illustrate how varying bridge conditions can be modeled using BNs. The sample bridge is most closely represented by Case 5 with the individual girder P_f = 1.64x10^{-3} and β = 2.94 and bridge system P_f = 3.29x10^{-3} and β = 2.72. As expected, the series system reliability is less than for the individual girder. Referring to the accepted design load ratings (RF_{inv} = 0.84 and RF_{oper} = 1.09) for this bridge, several general comparisons are possible. If looking at the individual girder level, since the reliability index was found to be above 2.5 and less than 3.5, then the inventory rating factor would be expected to be less than 1.0, and the operating rating would likewise be expected to be greater than 1.0. Similar comments can be made for the system level since the reliability index similarly lies between 2.5 and 3.5. The following section will describe a direct method used to determine rating factors with BNs.

Table 3.4: BN Case examples

Case no.	Structure[a] type	Defect[b] location	Defect CS	Girder P_f	Girder β_{calc}	Girder[c] β_{P_f}	Bridge[d] P_f	Bridge[c,d] β_{P_f}
1	girder	g1: member	CS1	$5.60\text{x}10^{-4}$	3.25	3.26	–	–
2	girder	g1: member	CS3	$5.98\text{x}10^{-4}$	3.24	3.24	–	–
3	girder	g1: segment	CS1,2,3	$1.34\text{x}10^{-3}$	–	3.00	–	–
4	girder	g1: midspan	CS3	$1.64\text{x}10^{-3}$	–	2.94	–	–
5	bridge	g1: midspan	CS3	$1.64\text{x}10^{-3}$	–	2.94	$3.29\text{x}10^{-3}$	2.72
		g2: midspan	CS3	$1.64\text{x}10^{-3}$	–	2.94	–	–
6	bridge	g1: segment	CS1,2,3	$1.34\text{x}10^{-3}$	–	3.00	$1.94\text{x}10^{-3}$	2.89
		g2: member	CS3	$5.98\text{x}10^{-4}$	3.24	3.24	–	–

[a] Structure type - girder considers one individual girder; Structure type - bridge uses a series system of girder pair supporting deck with assumed $P_{f_{deck}} = 3.40\text{x}10^{-6}$ and $\beta_{deck} = 4.50$.

[b] Defect location is indicated as either member (defect is located along entire length), midspan (defect is centered at midspan; all other areas are assumed CS1) or segment (CS1,2,3 defects are distributed along the girder).

[c] Girder and bridge reliability indexes estimated using $\beta = -\Phi^{-1}(P_f)$.

[d] Girder and bridge P_f and β shown are the most conservative values in the calculated intervals for series system.

3.9 Estimating Element and System Rating Factors

Rating factors are used to provide reliability information for a given structural element. Inventory and operating rating factors are used to convey two levels of structural reliability. The Inventory RF gives the user an idea of how close the element is to having a reliability index of 3.5. If $RF_{inv} = 1.0$, then the intent is for the element to provide a reliability index of 3.5. If the factor increases, then the structure is considered more reliable and if the factor decreases, then the structure is considered to be less reliable. The similar description can be given for the Operating RF in that if $RF_{oper} = 1.0$, then the intent is for the element to provide a reliability index of 2.5.

The BN can directly provide a measure of the reliability of the element by giving the user a value of P_f and β directly. The previous BNs have used an HL-93 design live load. If the live load is scaled, then this effectively becomes a rating factor for the

element being modeled. If the live load is scaled such that the reliability index is 3.5, then that scaling factor is effectively the inventory rating factor, RF_{inv}. Similarly, if the live load is scaled so that the resultant reliability index is 2.5, then the scaling factor is the operating rating factor, RF_{oper}. Scaling factors were applied to networks with baseline CS1 and example CS3 defects such that reliability indexes of 2.5 and 3.5 were determined. The rating factors for Cases 1,2 and 5 are shown in Table 3.5.

There are several ways to interpret these results. The first is to use the reliability indexes derived from the probability of failure values to estimate the member rating factors. For example, from column 1 of Table 3.5, $RF_{inv}^{CS1,P_f} = 0.89$ and $RF_{oper}^{CS1,P_f} = 1.29$ since the β_{P_f} reliability indexes, for CS1 defects, are at or near the target values, which are found in column 3. The primary disadvantage of this approach is that the limit state distribution is assumed to be normal. In our examples, all of the distributions are normal, so using the relation $\beta = -\Phi^{-1}(P_f)$ is not a burden. However, if any of the nodes are defined using other distributions, such as lognormal, then our ability to directly determine the reliability index from the network becomes an advantage.

That leads to the second interpretation which is to calculate the reliability index directly using the definition of reliability index: $\beta = \mu_g/\sigma_g$ where μ_g and σ_g are the mean and standard deviation, respectively, of the limit state function, $g(R, Q)$. When the definition is used, then $RF_{inv}^{CS1,calc} = 0.91$ and $RF_{oper}^{CS1,calc} = 1.27$. Similar reliability indexes are provided in the table from the network with example CS3 defects: $RF_{inv}^{CS3,P_f} = 0.88$, $RF_{oper}^{CS3,P_f} = 1.29$, $RF_{inv}^{CS3,calc} = 0.91$ and $RF_{oper}^{CS3,calc} = 1.27$.

This process can be extended to the system level assuming series elements. More details regarding this can be found in the Appendix. Combining series elements can yield a bounding interval for both the system P_f and β so that a range of rating factors will be the result. The series system is defined to be 2 girders and the deck (Case 5). The conservative approach would then be to take the lower value for both inventory and

operating rating factors which are $RF_{inv,sys}^{CS3,P_f}$ = 0.77 and $RF_{oper,sys}^{CS3,P_f}$ = 1.16. This once again exhibits the expected behavior where the series system reliability is less than that of the individual girder and would therefore have a lower capacity (for a given reliability index) and lower rating factor.

During the most recent load rating performed for the example bridge, the design rating factors were determined to be RF_{inv} = 0.84 and RF_{oper} = 1.09. These values assume reduced capacity due to redundancy and condition issues per the MBE. If Case 5 (Table 3.5) conditions are representative of the actual bridge conditions and the assumed deck conditions are appropriate, then the BN results indicate that the bridge, as a system, has less inventory capacity than indicated by conventional inventory rating factor calculations (RF_{inv} = 0.77 vs 0.84). This may be due to the current AASHTO code assuming distributions with differing attributes. For example, steel reinforcement prior to the 1970s was assumed to have a relatively high coefficient of variation. But, since that period, the variation has decreased due to recycled steel providing more uniform properties Nowak et al. 2012. The results presented so far in this paper have used steel reinforcement properties representative of the era in which the example bridge was built (prior to the 1970s). Refer to Table 3.1 for the material properties used to model the example bridge. Also, the bridge, as a system, has slightly more operating capacity than indicated by conventional operating factor calculations (RF_{inv} = 1.16 vs 1.09). The 1949 example bridge was probably designed using the 1944 American Association of State Highway Officials (AASHTO) Bridge Design Specification (4th edition). The resultant reliability indexes of previous specifications can range from as low as 2.0 to as high as 4.5 with some additional variability due to span length. Shorter span bridges may have been designed with inherent reliability indexes of 1.5, but generally aren't found to be unsafe.

Table 3.5: Reliability index results for networks with girder example defects and scaled live loads. Bold indicates values near target reliability indexes of 2.5 and 3.5 representative of operating and inventory rating factors. Using standard practice from the MBE provides inventory and operating rating factors of 0.84 and 1.09, respectively.

	CS1 Defects (Case 1)			CS3 Defects (Case 2)			CS3 Defects (Case 5)	
Scale (RF)	β_{calc}	β_{P_f}	P_f	β_{calc}	β_{P_f}	P_f	β_{P_f}	P_f
0.77	3.93	3.77	8.16x10^{-5}	3.92	3.75	8.79x10^{-5}	**3.50**	2.36x10^{-4}
0.88	3.60	3.52	2.16x10^{-4}	3.59	**3.50**	2.32x10^{-4}	3.22	6.35x10^{-4}
0.89	3.57	**3.50**	2.36x10^{-4}	3.56	3.48	2.53x10^{-4}	3.20	6.90x10^{-4}
0.91	**3.51**	3.45	2.77x10^{-4}	**3.50**	3.43	2.97x10^{-4}	3.15	8.08x10^{-4}
1.16	2.80	2.85	2.16x10^{-3}	2.79	2.84	2.29x10^{-3}	**2.50**	6.29x10^{-3}
1.27	**2.51**	2.56	5.23x10^{-3}	**2.49**	2.54	5.53x10^{-3}	2.16	1.53x10^{-3}
1.29	2.45	**2.51**	6.12x10^{-3}	2.44	**2.49**	6.47x10^{-3}	2.10	1.79x10^{-3}

3.10 Comparison of Current LRFD Girder Design and Bayesian Network

A final example will be presented that considers a contemporary RC girder bridge designed using the current LRFD code AASHTO 2020. The new bridge uses the same girder cross section dimensions as the existing example two-girder bridge, but uses modern reinforcement steel with a higher nominal yield strength and lower yield strength COV as shown in Table 3.1. Reinforcement is placed in the same vertical locations as the example bridge, with 3,871.0 mm^2 (6 in^2) in the bottom layer, and 3,225.8 mm^2 (5 in^2) in the next layer. Additionally, the new bridge is configured with 4 girders using 1.75 m (5.75 ft) c-c spacing. This results in a more structurally redundant bridge system when compared to the example bridge. The bridge was designed using unity load modifiers except for operational importance (η_I = 1.05), HL-93 live design loads, f'_c = 4 ksi, and f_y = 60 ksi. Parameters used related to LRFR rating included ϕ_c = 1.0, ϕ_s = 1.0 to reflect a new, redundant bridge. The bridge girder was designed with a factored nominal capacity of ϕM_n = 5,172.4 kN·m (3,815 kip·ft). Total factored loads used in the design

were M_u = 4,929.7 kN·m (3,636 kip·ft). The calculated rating factors using Eq. 3.4 were determined to be RF_{inv} = 1.12 and RF_{oper} = 1.45.

Using the methods already presented, the BN for the 4-girder RC bridge was assembled, and the girder and bridge system probability of failure, reliability indexes, and rating factors were determined. For this bridge system, the four girders are considered to be parallel elements, and as such, the rating factors and intervals for both P_f and β were determined. Refer to the Appendix for more information regarding a parallel system of elements.

For the inventory factor: $RF_{inv_{P_f}}$ = 1.77, $2.63\text{x}10^{-15} < P_{f_{sys}} < 2.26\text{x}10^{-4}$, and $3.51 < \beta_{P_{f_{sys}}} < 7.82$. For the operating factor: $RF_{oper_{P_f}}$ = 2.15, $1.60\text{x}10^{-9} < P_{f_{sys}} < 6.32\text{x}10^{-3}$, and $2.49 < \beta_{P_{f_{sys}}} < 5.92$. Since the girders would be constructed using the same materials and techniques, the capacities could be assumed to be highly dependent (correlated). The would lead us to the higher bound of the P_f interval, so that $\beta_{inv_{sys}}$ = 3.51 and $\beta_{oper_{sys}}$ = 2.49. In spite of using the higher limit of the interval, all of this results in relatively higher rating factors for the bridge structure when compared to conventional methods (RF_{inv} = 1.77 vs 1.12 and RF_{oper} = 2.15 vs 1.45) suggesting that current design practice may be overly conservative for this type of simple RC structure.

This type of analysis using BNs can be very sensitive to the live and dead load distributions being used. To illustrate this, another LL distribution can be substituted where the live load bias factor λ = 1.60 is used (vs 1.40) with a BN to determine the resulting rating factors. This bias factor can be justified by using data from more recent research Nowak and Iatsko 2017 using a larger weigh-in-motion database. When accounting for daily truck traffic, the bias factor ranges from 1.42–1.60 for a 15.2 m (50 ft) bridge, for maximum 75-year moments. When using the higher bias factor, and still using COV = 0.18, the following results were found for the rating factors: $RF_{inv_{P_f}}$ = 1.50 and $RF_{oper_{P_f}}$ = 1.83. With the increase of bias factor the structural reliability is

reduced, but the rating factors are still greater than those found using LRFR.

3.11 Conclusions

Although load ratings can be viewed to be a deterministic method to estimate allowable loads on a bridge, this is not entirely the case since the LRFR/LRFD processes use load and resistance factors which are based on probabilistic methods. However, using the LRFD design methodology is extremely helpful during the design process in that design iterations can be performed relatively quickly and easily. Nonetheless, once the design process is finished, and the bridge structure is constructed and is in service, then a different evaluation process may be appropriate. In this study, BNs were used to directly account for a limited set of defects and to produce rating factors that represent a desired structural reliability. BNs can also be used to inform a more general asset management tool since estimates of the probability of failure for all managed assets can be compared objectively when prioritizing maintenance and replacement efforts. The LRFR method uses a broad stroke approach to account for lack of redundancy and component condition. BNs provide a method to directly account for these concerns without arbitrarily accommodating them. The results presented show that when using conventional LRFR rating, the inventory rating for an existing, simple two-girder RC bridge may be slightly overstated, and the operating rating may be slightly understated. However, the reliability of a new four-girder RC bridge is more significantly understated. The differences may be due to the approximation methods used when determining the load and resistance factors used with LRFD design. This type of modeling using BNs could be extended by including different types of building materials, including steel and prestressed concrete. Additionally, understanding the impact of material deterioration on steel section loss would be a natural improvement to the models.

The advantages of using BNs for reliability analysis include the direct inclusion of defects found during bridge inspections, flexibility of the types of live loads being used, and the direct determination of rating factors. Also, additional information from NDT measurements can directly be incorporated into BNs, with their errors and uncertainties appropriately captured. The disadvantages of this methodology include significant dependence on determining appropriate statistical parameters, discretizing the distributions in the networks requiring mindful management so as not to improperly skew results, and the significant effort needed to understand the impact of defects through expert opinion.

3.12 Appendix - Details of Bayesian Network Examples

3.12.1 Case 1 - Individual Girder with CS1 Defects

To account for various types of defects, the BN must be modified. As previously stated, BNs in the current work include the effects of defects by reducing the compressive strength of concrete. The implementation of this is shown in Fig. 3.5. This example shows all defects to be at the CS1 level, with the initial concrete average strength to be 26.54 MPa (3.85 ksi). After using the provided defects and CPTs, the network provides a reduced concrete compressive strength of 25.23 MPa (3.66 ksi). This new *Reduced* f_c' node is then used in the moment BN which ultimately yields the girder probability of failure. The CS1 state is assumed to be uniformly present along the girder and the moment present at midspan is used. As shown in Table 3.4, P_f = 5.60x10^{-4} with $\beta = -\Phi^{-1}(5.60x10^{-4}) = 3.26$. Compare this to the model with no defects being modeled (Fig. 3.3) with P_f = 5.57x10^{-4} with $\beta = -\Phi^{-1}(5.57x10^{-4}) = 3.26$. There is very little difference between the BNs, but a slight increase in P_f is expected since, even with CS1 defects, there is a slight impact on f_c', resulting in a slight decrease in structural reliability.

3.12.2 Case 2 - Individual Girder with CS3 Defects

Contrast the previous example to another situation where the inspector has found CS3 defects along the girder length. Using the BN, after the defects are entered as CS3, the reduced compressive strength is found to have a mean and standard deviation of 19.58 MPa (2.84 ksi) and 4.34 MPa (0.63 ksi), respectively, as shown in Fig. 3.6.

As already shown, a primary benefit of using BNs is that new information can be entered into the network in the form of inspection findings. Using the BN as previously

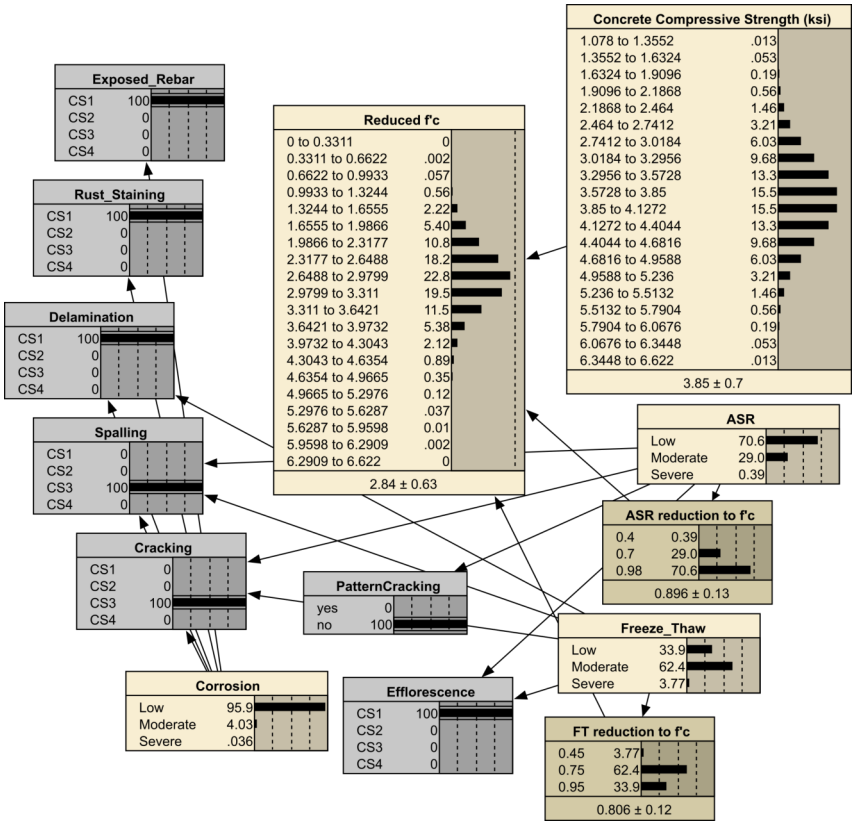

Figure 3.6: Example network with reduced concrete compressive strength due to defects with spalling and cracking assumed at condition state CS3. Initial concrete compressive strength has mean and standard deviation of 26.54 MPa (3.85 ksi) and 4.84 MPa (0.702 ksi), respectively. The *Reduced* f_c' node provides final concrete compressive strength after CS3 defect findings are entered, and has mean and standard deviation of 19.58 MPa (2.84 ksi) and 4.34 MPa (0.630 ksi), respectively.

described, the deterioration modes can also be predicted. From Fig. 3.6, once the CS3 defects are entered, the network is also telling us that there is a 29% probability that the concrete has Moderate ASR. Also, there is a 62% probability that the concrete has Moderate levels of FT. This provides the inspector additional information as to what recommendations could be provided to the bridge owner. In this case, water drainage might be a problem at this specific location, or possibly the existing cracking has not been suitably repaired allowing ongoing damage to occur.

The results from the BN with CS3 defects are provided in Table 3.4, where P_f = 5.98x10^{-4}, with $\beta_{calc} = \mu_g / \sigma_g$ = 3.24, and $\beta_{P_f} = -\Phi(5.98\text{x}10^{-4})$ = 3.24. Although the defects caused only a small decrease in structural reliability as compared to Case 1, the network is reacting as expected due to the reduced concrete strength. The reduction is most likely minimized due to the relatively large effective flange width being used.

3.12.3 Case 3 - Individual Girder with Multiple Defects

Examples provided so far have only illustrated defects that are considered uniform along the member of interest. To support the presence of multiple defects, the member can be thought of as a series of individual segments Groeneveld et al. 2021. The segments are selected so that the defect types and severity are constant along the length of a defined segment. If the member is prismatic, and reinforcing steel does not vary along the length of the member, then the moment capacity is also constant in the segment. However, the live load is mobile resulting in the moment load effect not being constant along the segment. A load marching algorithm is used to determine the maximum total moment caused by the dead load and moving truck load for each segment. The process used to segment a member is illustrated in Fig. 3.7. An example would be to refer to defects 1 and 3 which are present in Segment 3. Although both defects are present outside of

Segment 3, the BN representing Segment 3 will only be concerned with defects 1 and 3 between points X_7 and X_2. After the maximum moment is determined, the defects are applied resulting in the final BN with the final limit state node. This process is repeated for all previously defined segments, so the end result is a set of vectors representing P_{f_i}, μ_{g_i}, and σ_{g_i} which are the probability of failure, limit state mean, and limit state standard deviation for each individual segment, S_i.

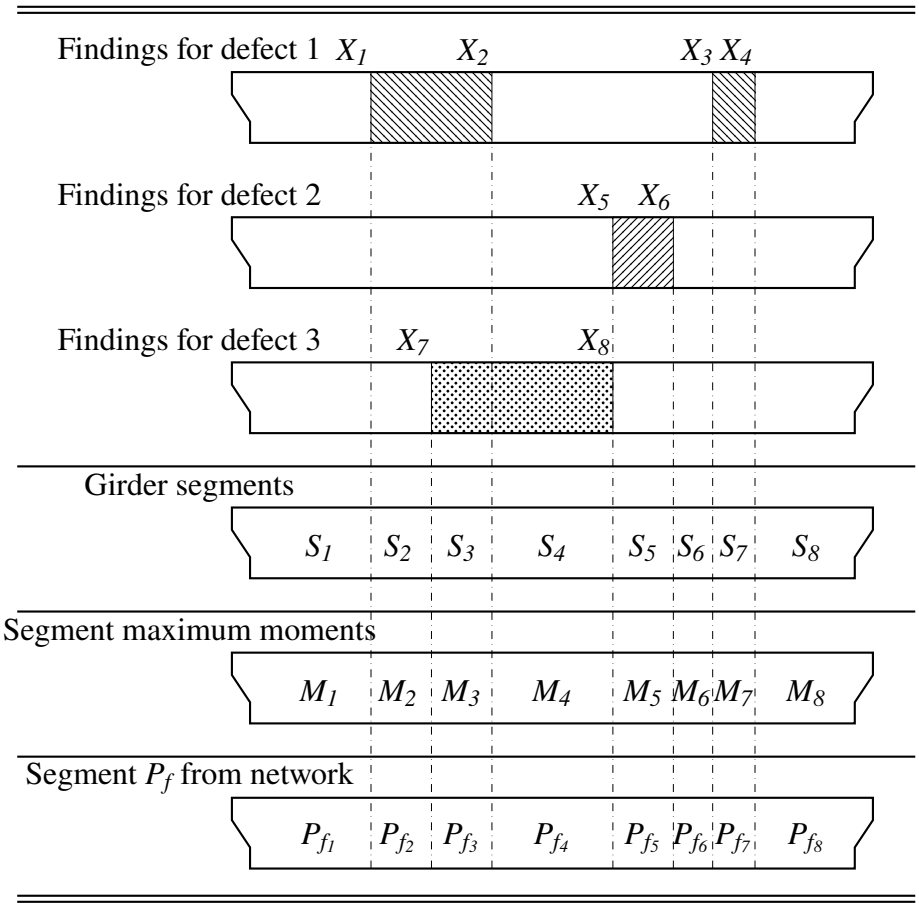

Figure 3.7: Illustration of defect segmentation of girder with example defects affecting moment capacity

The individual segments are then considered a series system, or a weakest-link system, because if the weakest segment fails, then the entire member would fail. In our structural system, the weakest-link would be the segment with the highest probability of

failure, or the lowest reliability index. But, we have the question of whether the individual segments, and capacities, are to be considered dependent or independent of each other. If there exists positive correlation between some or all of the segments, then determining the structural reliability of the system can be quite difficult. To bound the problem Nowak and Collins 2012, Ayyub and McCuen 2003, the segments can be viewed as fully correlated (dependent) resulting in a lower bound, and as fully uncorrelated (independent) resulting in an upper bound. This can be expressed as:

$$\max_{1\leq i\leq n} P_{f_i} < P_{f_{sys}} < 1 - \prod_{i=1}^{n} \left(1 - P_{f_i}\right) \tag{3.9}$$

A similar expression can also be used if the elements are parallel. As before, to bound the problem, the segments can be viewed as fully uncorrelated (independent) resulting in a lower bound, and as fully correlated (dependent) resulting in an upper bound. This can be expressed as:

$$\prod_{i=1}^{n} P_{f_i} < P_{f_{sys}} < \min_{1\leq i\leq n} P_{f_i} \tag{3.10}$$

Both of these equations will be used when combining series and parallel elements of a bridge system.

3.12.4 Example Girder Segmentation

Fig. 3.7 can be used as an example of the segmentation process. The assumed defect types, severity, and locations are provided in Table 3.6. Three defects are being considered. Defect 1 is the presence of pattern cracking and is being placed at two separate areas (0.2S to 0.4S and 0.75S to 0.82S). Defect 2 is spalling located at one area (0.6S to 0.7S), and defect 3 is efflorescence located along 0.3S to 0.6S. In this usage, S

Table 3.6: Girder segmentation example parameters

	Location (% Span)					
Segment no.	Begin	End	Defect no.	Defect state	Defect type	P_f
1	0.0S	0.2S	-	CS1	All	2.36x10^{-8}
2	0.2S	0.3S	1	present	Pattern Cracking	4.00x10^{-5}
3	0.3S	0.4S	1	present	Pattern Cracking	3.52x10^{-4}
			3	CS2	Efflorescence	
4	0.4S	0.6S	3	CS2	Efflorescence	5.56x10^{-4}
5	0.6S	0.7S	2	CS3	Spalling	3.53x10^{-4}
6	0.7S	0.75S	-	CS1	All	4.03x10^{-5}
7	0.75S	0.82S	1	present	Pattern Cracking	2.63x10^{-6}
8	0.82S	1.0S	-	CS1	All	9.90x10^{-10}

is taken to be the span of the girder between bearing centers. Table 3.6 provides all the segmentation data, but also the final probabilities of failure for each individual segments. The girder is always assumed to be at a base CS1 state for all defects which means the defect is considered benign or could not even be found. However, since the moment load effects will be different for each segment, all portions of the girder which are considered at a CS1 state are not required to share the same probability of failure. This can be seen for segments 1, 6, and 8.

Once this information is in hand for each segment, then an interval representing the girder probability of failure can be determined. Using Eq. 3.9, the girder P_f can be estimated to be within the interval of 5.56x10^{-4} < P_f < 1.34x10^{-3}. If the assumption that all distributions are normal is used again where $\beta = -\Phi^{-1}(P_f)$, then the estimated reliability index will be bounded by the interval of 3.00 < β_{P_f} < 3.26. To be conservative, the lower reliability index could be chosen as the representative index.

3.12.5 Case 4 - Individual Girder with CS3 Midspan Defects

Case 4 is similar to the conditions found at the example bridge (Fig. 3.2). Assume that a spall was found and determined to be 178 mm (7 in) in diameter, and nearby cracking was measured to be around 2.54 mm (0.1 in) wide. According to the MBEI AASHTO 2013, both of these defects should be classified as CS3. The defects are centered around the girder midspan and the affected area is 1.63 m (5.35 ft) in length. Using the method described in Case 3, the girder can be thought of as 3 segments with segments 1 & 3 having base CS1 defects, and the middle segment with the discovered CS3 defects.

Once this information is available for the 3 segments, then an interval representing the girder probability of failure can be determined. Using Eq. 3.9, the girder P_f can be estimated to be within the interval of $6.00\text{x}10^{-4} < P_f < 1.64\text{x}10^{-3}$. If the assumption that all distributions are normal is used again where $\beta = -\Phi^{-1}(P_f)$, then the estimated reliability index will be bounded by the interval of $2.94 < \beta_{P_f} < 3.24$. To be conservative, the lower reliability index could be chosen as the representative index. Although both Cases 3 & 4 have CS1 and CS3 defects, Case 4 has a more severe defect midspan (with the highest moment load), resulting in a slightly higher P_f and reduced structural reliability.

3.12.6 Case 5 - Girder Pair with CS1 Defects and Deck

A bridge system probability of failure can then be estimated if we use a pair of the individual girders discussed in Case 4. To include the deck, having the probability of failure of the deck would be ideal. But, since this is not readily available, an estimate of $P_f = 3.40\text{x}10^{-6}$ can be used which corresponds to a reliability index $\beta = 4.50$. Typical bridge load ratings exclude the bridge deck, so to illustrate the ability to include the deck, an arbitrary, relatively high value for the deck reliability was chosen. As in Case 4, the

girders will be considered as 3 segments and the girders and deck will all be considered elements in series because a failure of either girder, or the deck, would result in the failure, or loss of functionality, of the bridge. Again using Eq. 3.9 to find an interval yields: $1.64\text{x}10^{-3} < P_{f_{sys}} < 3.29\text{x}10^{-3}$ with the estimated interval for the reliability index: $2.72 < \beta_{P_f} < 2.94$. When compared to Case 4 with individual girders having CS1/CS3 defects, the two-girder series system has a reduced structural reliability.

3.12.7 Case 6 - Girder Pair with CS1,2,3 Defects and Deck

The last example is another general case where a pair of girders are modeled, but the defect condition states are different. The girders described in Cases 2 & 3 are used, in addition to the hypothetical deck. The approach is identical as described in Case 5, but different girder conditions are used. Using Eq. 3.9 to find an interval yields: $1.34\text{x}10^{-3} < P_{f_{sys}} < 1.94\text{x}10^{-3}$ with the estimated interval for the reliability index: $2.89 < \beta_{P_f} < 3.00$.

3.13 Data Availability Statement

Some or all data, models, or code that support the findings of this study are available from the corresponding author upon reasonable request. Applicable items are Netica BN models.

3.14 Acknowledgments

The authors thank the U.S. Army Corps of Engineers for the use of as-built data for bridges in the current inventory. Additionally, support from the U.S. Army and Corps (through participation in ERDC-University and funding of Projects 476923 & 154349) is acknowledged.

Edgardo Ruiz was formerly at the U.S. Army Engineer Research and Development Center, Vicksburg, MS, at the time of this research and is now affiliated with Fickett Structural Solutions, Inc.

3.15 References

American Association of State Highway Officials (AASHTO) (2011). *Manual for Bridge Evaluation*. AASHTO, Washington, D.C., 2nd edition.

American Association of State Highway Officials (AASHTO) (2013). *Manual for Bridge Element Inspection*. AASHTO, Washington, D.C., 1st edition. 2015 interims.

American Association of State Highway Officials (AASHTO) (2014). *LRFD Bridge Design Specifications*. AASHTO, Washington, D.C., 7th edition.

American Association of State Highway Officials (AASHTO) (2020). *LRFD Bridge Design Specifications*. AASHTO, Washington, D.C., 9th edition.

American Concrete Institute (ACI) (2013). *Report on Nondestructive Test Methods for Evaluation of Concrete in Structures - 228.2R*. ACI, Farmington Hills, MI.

American Concrete Institute (ACI) (2019). *Report on Methods for Estimating In-Place Concrete Strength - 228.1R*. ACI, Farmington Hills, MI.

Ayyub, B. and McCuen, R. (2003). *Probability, statistics, and reliability for engineers and scientists*. Chapman & Hall/CRC Press, Boca Raton, FL.

Bertola, N., Henriques, G., Schumacher, T., and Brühwiler, E. (2022). "Engineering of existing structures: The need and place for non-destructive evaluation." *International Symposium on Nondestructive Testing in Civil Engineering*, Zurich, Switzerland. (August 16-18, 2022).

Campbell, L., Snyder, L., Whitehead, J., Connor, R., and Lloyd, J. (2019). "Probability of detection study for visual inspection of steel bridges: Volume 2 - full project report."

Joint Transportation Research Program Publication FHWA/IN/JTRP-2019/22, Indiana Dept. of Transportation.

Ellingwood, B., Galambos, T., McGregor, J., and Cornell, C. (1980). *Development of a probability based load criterion for american national standard A58*. U.S. Department of Commerce, National Bureau of Standards, Washington, D.C. NBS Special Report 577.

Estes, A. and Frangopol, D. (2005). "Load rating versus reliability analysis." *Journal of Structural Engineering*, 131(5), 843–847.

Federal Highway Administration (FHWA) (2020). *National Bridge Inventory*. LTBP InfoBridge: Analytics, Washington, D.C., <https://infobridge.fhwa.dot.gov/BarStackChart> (Jan. 3, 2022).

Groeneveld, A., Wood, S., Ruiz, E., and Roberts, J. (2021). "Estimating bridge reliability by using bayesian networks." *U.S. Army Corps of Engineers Engineer (USACE) Research and Development Center (ERDC)*.

Hanjari, L., Utgenannt, P., and Lundren, K. (2008). "Experimental study of the material and bond properties of frost-damaged concrete." *Cement and Concrete Research*, 41(3), 244–54.

Heckerman, D. and Wellman, M. P. (1995). "Bayesian networks." *Communications of the ACM*, 38(3), 27–30.

Ji, X., Song, Y., and Liu, Y. (2008). "Effect of freeze-thaw cycles on bond strength between steel bars and concrete." *Journal of Wuhan University of Technology-Materials Science Edition*, 23(4), 584–88.

Karshenas, A. and Naghavi, B. (2020). “Investigating available state-of-the-art technology for determining needed information for bridge rating strategies.” *Report no.*, Louisiana Department of Transportation and Development.

Küttenbaum, S., Braml, T., Taffe, A., Keßler, S., and Maack, S. (2021). “Reliability assessment of existing structures using results of nondestructive testing.” *Structural Concrete*, 22(5), 2895–2915.

LeBeau, K. (2008). “A bi-directional load rating model of the flexural response of a prestressed concrete bridge beam element.” Ph.D. thesis, Northeastern University, Boston, MA.

Lequesne, R. and Collins, W. (2020). “Load rating reinforced concrete bridges without plans: State-of-the-practice.” *ACI Symposium Publication* (http://dx.doi.org/10.14359/51725938).

Moore, M., Pares, B., Graybeal, B., Rolander, D., Washer, G., and Wiss, J. (2001). “Reliability of visual inspection for highway bridges volume 1.” *Report No. FHWA-RD-01-105*, Turner-Fairbank Highway Research Center.

Norsys (2019). *Netica 6.07*. Norsys Software Corp, Vancouver, Canada.

Nowak, A. (1995). “Calibration of LRFD bridge code.” *Journal of Structural Engineering*, 121(8), 1245–1251.

Nowak, A. and Collins, K. (2012). *Reliability of Structures*. CRC Press.

Nowak, A. and Iatsko, O. (2017). “Revised load and resistance factors for the AASHTO LRFD bridge design specifications.” *PCI Journal*, 62(3), 46–58.

Nowak, A., Rakoczy, A., and Szeliga, E. (2012). "Revised statistical resistance models for r/c structural components." *American Concrete Institute Special Publication*, 284, 1–16.

Nowak, A. and Szerszen, M. (2000). "Structural reliability as applied to highway bridges." *Progress in Structural Engineering and Materials*, 2(2), 218–284.

Nowak, A., Yamani, A., and Tabsh, S. (1994). "Probabilistic models for resistance of concrete bridge girders." *American Concrete Institute Structural Journal*, 91(3), 269–276.

Pradhan, M., Henrion, M., Provan, G., Del Favero, B., and Huang, K. (1996). "The sensitivity of belief networks to imprecise probabilities: an experimental investigation." *Artificial Intelligence*, 85(1-2), 363–397.

Roberts, J., Ruiz, E., Groeneveld, A., and Pérez-Gracia, R. (2019). "Use of bayesian networks for inferences on bridge safety." *Proceedings of the 98th Annual Meeting of the Transportation Research Board*, Washington, DC. (Jan 13-17, 2019). Presentation no. 19-04278.

Seijas-Macías, A. and Oliveira, A. (2012). "An approach to distributions of the product of two normal variables." *Discussiones Mathematicae Probability and Statistics*, 87–99 (http://dx.doi.org/10.7151/dmps.1146).

Shang, H., Cao, W., and Wang, B. (2014). "Effect of fast freeze-thaw cycles on mechanical properties of ordinary air-entrained concrete." *The Scientific World Journal* (http://dx.doi.org/10.1155/2014/923032).

Chapter Four:

Estimating Prestressed Concrete Bridge Reliability and Rating Factors Using Bayesian Networks with an Application to a Bridge Made Continuous for Live Load

This paper was submitted to the *Practice Periodical on Structural Design and Construction* on 28 June 2023 and is under review.

Jeffery M. Roberts[1], Thomas Schumacher[2], Andrew B. Groeneveld[3], Stephanie G. Wood[4], and Edgardo Ruiz[5]

The authors contributed as follows: study conception and design: J.M. Roberts, A.B. Groeneveld, S.G. Wood, E. Ruiz; analysis and interpretation of results: J.M. Roberts, T. Schumacher; draft manuscript preparation: J.M. Roberts, T. Schumacher.

[1]Ph.D. Candidate, Dept. of Civil and Environmental Engineering, Portland State University, Portland, OR 97201. Structural Engineer, U.S. Army Corps of Engineers, Portland District, 333 SW 1st Ave, Portland, OR 97204 (corresponding author). ORCID: https://orcid.org/0000-0002-3505-0580. Email: jeffery.m.roberts@usace.army.mil

[2]Associate Professor, Dept. of Civil and Environmental Engineering, Portland State University, 1930 SW 4th Ave., Portland, OR 97201. ORCID: https://orcid.org/0000-0003-0118-9119. Email: thomas.schumacher@pdx.edu

[3]Research Civil Engineer, U.S. Army Engineer Research and Development Center, Geotechnical and Structures Laboratory, 3909 Halls Ferry Road, Vicksburg, MS 39180, Email: andrew.b.groeneveld@usace.army.mil

[4]Research Civil Engineer, U.S. Army Engineer Research and Development Center, Geotechnical and Structures Laboratory, Vicksburg, MS 39180. Email: stephanie.g.wood@usace.army.mil

[5]Senior Project Manager, Fickett Structural Solutions, Inc., Orlando, FL 32832. ORCID: https://orcid.org/0000-0002-3718-8321. Email: eruiz@fickettinc.com

4 Chapter Four: Estimating Prestressed Concrete Bridge Reliability and Rating Factors Using Bayesian Networks with an Application to a Bridge Made Continuous for Live Load

Jeffery M. Roberts, Thomas Schumacher, Andrew B. Groeneveld,
Stephanie G. Wood, and Edgardo Ruiz

4.1 Abstract

The bridge inspection process has multiple steps. One obvious element is for inspectors to identify defects in the main components of the structural system and assign condition ratings. These condition ratings are somewhat subjective since they are influenced by the experience of the inspector. In the current work, processes were developed for making inferences on the reliability of prestressed concrete (PC) girders with defects at the girder component level. The Bayesian network (BN) tools constructed in this study use simple structural mechanics to model the capacity of girders. Expert opinion is used to link defects that can be observed during inspections to underlying deterioration mechanisms. By linking these deterioration mechanisms with changes in mechanical properties, inferences on the reliability of a bridge can be made based on visual observation of defects. The BN can then be used to directly determine the rating factor (RF) of individual structural elements. Examples are provided using BNs to evaluate an existing older PC bridge currently behaving as two simply supported spans. The bridge is modeled using two scenarios with the spans acting as simply supported, and then also with the link block (continuity joint) repaired so that the spans are continuous for live load. The spans are considered simply supported for all dead load.

4.2 Introduction

According to 2022 National Bridge Inventory (NBI) data, there are over 620,000 bridges in use in the United States FHWA 2022. The most common material type currently being used is reinforced concrete (RC), at almost 42%, which includes both simply supported and continuous spans. The next most common material types are steel and prestressed concrete (PC), at 27.8% and 27.2%, respectively, of all U.S. bridges. There are also still some timber bridges being used that are included in the 2022 inventory, at 2.6%. Since all of these material types can deteriorate over time, bridge owners inspect each structure in order to find defects early and to improve the long-term performance of their bridges. Defects are as defined in the Manual for Bridge Element Inspection (MBEI) AASHTO 2013. However, the inspection process can be influenced by the subjective judgment of the team leader and each member of the inspection team. Inspection findings can vary between inspection teams and can also vary as a structure is inspected multiple times Campbell et al. 2019, Moore et al. 2001.

This paper illustrates the use of Bayesian Networks (BNs) to determine the structural reliability of PC members and to update the reliability as a result of inspection findings. The networks use simple structural mechanics and current design codes to model the capacity of prestressed girders. Expert elicitation Groeneveld et al. 2021, Roberts et al. 2023 is used to relate observable defects to deterioration mechanisms that impact the modeled compressive strength of concrete.

An example bridge designed and constructed with prestressed girders is used to illustrate the use of BNs and how they can be used to determine rating factors. The circa 1982 bridge located at a U.S. Army Corps of Engineers (USACE) dam project was last inspected in 2018 and has a 2019 load rating report. The load rating analysis was performed in accordance with then-current design AASHTO 2017 and rating AASHTO

2018 guidance. The rating factors, determined using both conventional methods and BNs, are compared. The example bridge, although originally intended to behave continuous with live load, is considered to currently have two simply supported spans because of damage to the link block (continuity joint). The bridge is examined using two scenarios with the spans acting as simply supported, and also with the link block repaired at the mid-support so that the spans are continuous for live load. The spans are still considered simply supported for all dead load.

4.3 Bayesian Networks

A Bayesian Network (BN) is a graphical representation of a set of variables that highlights the parent/child relationship and provides the probability of interaction between nodes through the use of conditional probability tables (CPTs). A BN is a directed acyclic graph (DAG) where nodes (variables) can be connected using unidirectional arcs (edges). There are no closed loops within a DAG. A BN example illustrating a model of a prestressed girder is shown in Fig. 4.1 where the network nodes have analogous variables in Eqs. 4.2-4.5. There are four parent nodes for the moment capacity (M), and two parent nodes for the total load node (MQ). These two nodes (M and MQ) are then parent nodes for the limit state node (gM). A more complete description for some of the nodes shown in Fig. 4.1 will be given throughout the paper. Also, the gM node is simply the difference between the parent nodes ($M - MQ$) so that the girder capacity is directly compared to the internal moments due to external live (MQ_LL) and dead (MQ_DL) loads. More information regarding BNs and concrete bridge structures can be found in Roberts et al. 2019, Groeneveld et al. 2021, and Roberts et al. 2023.

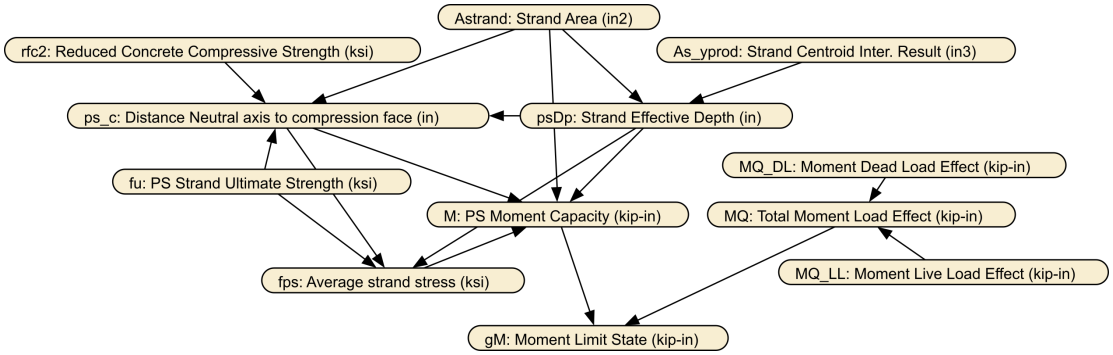

Figure 4.1: Example moment BN for PC girder. Live load effect (MQ_LL) values are changed to reflect continuous vs. simple spans. The same dead load effect (MQ_DL) values are used for both continuous and simple spans.

4.4 Reliability Analysis

All real structures are composed of elements with some unavoidable uncertainties related to design or construction Nowak and Collins 2012. With these innate uncertainties, there will always be a probability of failure (P_f) of at least one element of a structure since there is not a guarantee that the capacity always exceeds demand. A complement to the concept of probability of failure is the idea of a structure's reliability, where reliability can be defined to be $1 - P_f$. Therefore, to determine structural reliability, a definition of failure is needed. One simple way to view failure is to require that demand has exceeded capacity, or in terms of a limit function $g(R, Q) = R - Q$ where R represents the structural resistance (capacity) and Q represents the demand (load effect) on the structure. There are three outcomes. First, if $g > 0$, then the structural capacity exceeds the demand and failure is not occurring. Second, if $g = 0$, then demand is equal to the structural capacity and failure is forthcoming, whereas in the third outcome, $g < 0$, the demand exceeds capacity and failure is occurring. Therefore, in terms of the limit state, the probability of failure can be written as $P_f = P(g < 0)$. A concept useful when dealing with structural reliability is to quantitatively describe how far away the mean of

the limit state function is from the point of failure ($g = 0$) using the reliability index. For a limit state function, the reliability index, β, is defined to be μ_g/σ_g where μ_g and σ_g are the mean and standard deviation, respectively, of $g(R, Q)$. This represents the number of standard deviations that separate the mean and initiation of failure.

If normal distributions are used, then the probability of failure is related to the reliability index using the standard normal cumulative distribution function Φ: $P_f = \Phi(-\beta)$. The inverse is also helpful to determine the reliability index: $\beta = -\Phi^{-1}(P_f)$ where Φ^{-1} is the inverse of the standard normal cumulative distribution function.

4.5 Load Rating

The example bridge being used is a four-girder, two-span bridge that carries two lanes of traffic. The superstructure is made of a RC deck supported by four PC girders. The original construction in the early 1980s provided for a link block between longitudinally adjacent girders to make the arrangement structurally continuous for live load. Through the years, this link block has deteriorated and cracked to the point where the two spans are currently considered simply supported. Section and girder elevation drawings are shown in Figs. 4.2-4.3 in addition to a photo showing the bridge elevation in Fig. 4.4.

The Load and Resistance Factor Rating (LRFR) methodology AASHTO 2018 provides for both inventory and operating rating factors (RFs). The inventory RF uses LRFD strength limit states AASHTO 2020 that are calibrated to result in a target reliability of 3.5. Likewise, the operating RF results in a reduced target reliability of 2.5

For a given component, the LRFR load rating calculation, in its simplest form, is:

$$RF = \frac{\phi_C \phi_S (\phi R_n) - \gamma_{DL} DL}{\gamma_{LL} LL} \tag{4.1}$$

where ϕ_C is the component condition resistance factor, ϕ_S is the system resistance factor,

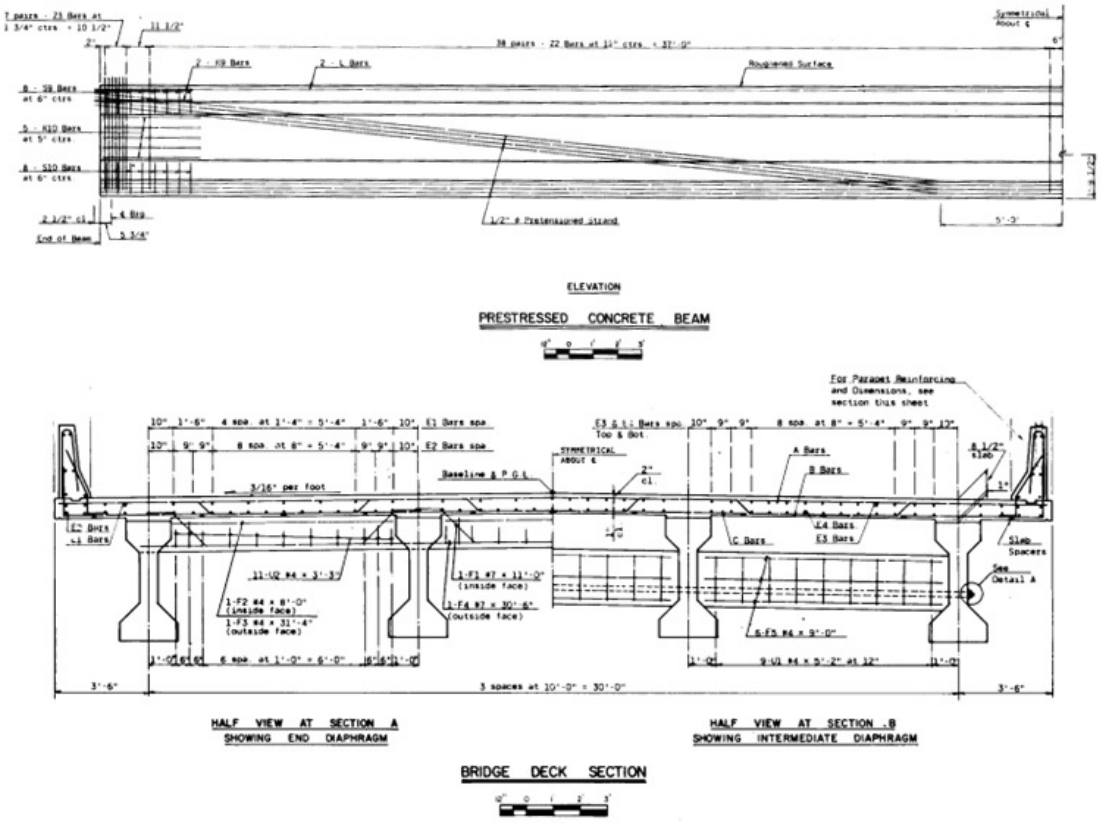

Figure 4.2: Example PC bridge section and main girder elevation views (reprinted with permission from USACE). Girders with bearing spacing of 23.8 m (78.04 ft) and girder spacing of 3.05 m (10.0 ft).

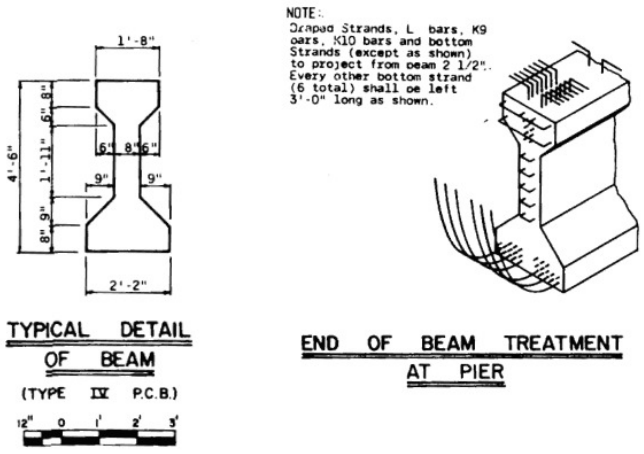

Figure 4.3: Example PC bridge girder sections (reprinted with permission from USACE). Extended prestressing strands at end of beam shown.

Figure 4.4: Photo of example bridge elevation showing link block (continuity joint) between spans (reprinted with permission from USACE). Insert photo shows closeup of link block deterioration.

ϕR_n is the factored capacity of the component, γ_{DL} and γ_{LL} represent the appropriate load factors for the dead and live loads, respectively, and DL and LL represent the dead load and live load effects, respectively. The live load is also calculated using impact and distribution factors. The rating factor resistance factors (ϕ_C and ϕ_S) are used to decrease the component capacity because of the assumed effects of degraded condition and lack of redundancy. The product $\phi_C \phi_S$ is not allowed to be less than 0.85. The RF represents the surplus capacity of a structural component after the dead load effect is accounted for. Since BNs directly integrate the uncertainties associated with node variables by using the bias factor, λ, and COV (defined in Table 4.1), these LRFR and LRFD resistance and load factors are not used when constructing a BN. The RF then acts as a live load scaling factor than can be selected so that a desired reliability is the result.

For the example bridge illustrated in Fig. 4.2, the most recent design rating factors were determined to be $RF_{inv} = 1.18$ and $RF_{oper} = 2.14$. The inventory RF is governed by the girder tension stress, and the operating RF is governed by the positive girder moment. The inventory RF for positive girder moment is 1.68, but does not govern. However, to simplify the implementation of the BN for the example girder, only moment

load effects are considered during this evaluation. Therefore, the rating factors being considered are $RF_{inv} = 1.68$ and $RF_{oper} = 2.14$. This rating used standard HL-93 design live loads. From the most recent inspection report, the superstructure was described to be in fair condition with the girders exhibiting some spalling and cracking but none resulting in a reduction of individual girder capacity. The link blocks between girders show exposed prestressing strands which would lead to a loss of structural continuity between the two spans. The rating resistance factors were taken to be $\phi_c = 1.0$ and $\phi_s = 1.0$. The flexure condition factor is used to account for the overall superstructure condition, but since the individual girders show no significant deterioration resulting in a reduced capacity, the condition factor was specified to be $\phi_c = 1.0$ for girders which are assumed to be simply supported. This discounts any assumption of the girders acting in unison. The flexure system factor reflects the fact that there are multiple longitudinal girders providing redundancy. For more information regarding RC bridge load ratings, refer to Roberts et al. 2023.

4.6 Bridges Made Continuous for Live Load

One step during the bridge design process is to determine if spans are to be simply supported or continuous if multiple spans are involved. Simply supported design is common for bridges using precast, PC girders. To minimize the number of expansion joints, another option is to use simply supported girders made continuous for live load by using individual continuity joints connecting adjacent girders. A disadvantage of this approach, however, is that creep, shrinkage, and thermal effects can create large positive moments Looney et al. 2021, Freyermuth 1969 in the continuity joint resulting in severe cracking and eventually the loss of moment transfer between spans. An example of this type of damage is shown on the example bridge in Fig. 4.4.

There is current research investigating how to improve the positive moment capacity Looney et al. 2021, Casey 2019 of these multiple span bridges by using Ultra High Performance Concrete (UHPC) in replacement continuity joints. If this repair method was applied to the example bridge and the original design intent of continuous span for live load was restored, then the next step would be to determine the new rating factor for the repaired structure. Creating a BN for this two-span bridge (both continuous and simply supported) would allow a comparison of rating factors representative of before vs. after repairs. The continuous behavior that is assumed in the continuous BNs is based upon load test results described in Looney et al. 2021. The spans were loaded at midspan using dump trucks with crushed stone. Since the tested spans were relatively short and produced small measured deflections, the results for all tested girders are not conclusive showing continuity after joint replacement. However, measured deflections were within 1 mm (0.04 in) of calculated deflections when assuming simple and continuous behavior. The conclusion can then be made that the joint replacement improved structural capacity by causing the spans to behave in a continuous manner.

One advantage of a continuous girder over multiple spans is to increase available capacity when compared to simply supported spans. However, in the case of the example bridge, all of the dead load including girder self-weight and deck dead load are supported by the existing simply supported spans. Only the live load would be supported by the bridge made continuous. The simply supported span (Fig. 4.5a) produces the highest positive moment for the girder, shown in Fig. 4.5d. The partial continuous bridge (Fig. 4.5b, with reduced stiffness for the link) has a lower positive moment, also shown in Fig. 4.5d. Assuming a consistent stiffness for the link (Fig. 4.5c), a slightly reduced positive moment is produced and is shown in Fig. 4.5d. This is only conceptual, but illustrates the possibility of not attaining a fully continuous girder. However, as shown in the figure, only around a 10% reduction in positive moment due to all loads is possible

since all dead load is supported by the original simply supported girders.

A further discussion of the idea of making bridges continuous for live load can also include historical design methodologies. A previous version (TxDOT 2001) of the Texas Department of Transportation (TxDOT) Bridge Design Manual (BDM) states that "the disadvantages outweigh the advantages of designing continuous for live load." The TxDOT BDM also states that "longer spans could more economically be achieved using slightly higher concrete strengths and 2 to 4 more prestressing strands."

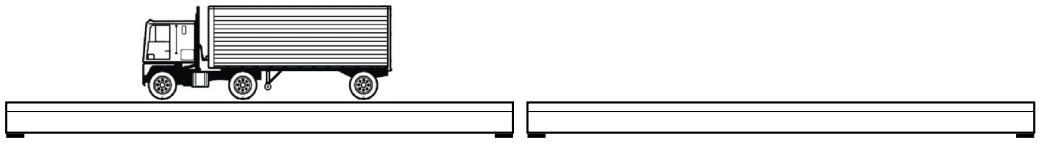

(a) Simply supported two-span bridge.

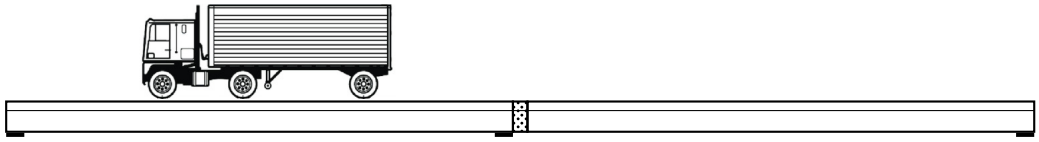

(b) Two-span bridge with link block between spans providing partial continuous beam behavior for live load.

(c) Two-span bridge with link block between spans providing continuous beam behavior for live load.

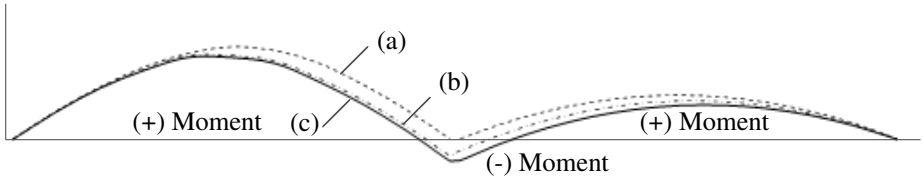

(d) Moment diagrams.

Figure 4.5: Qualitative moment diagrams showing the effect of AASHTO HL-93 design loads (lane loads not shown for simplicity; trucks not shown to scale). The simply supported span (a) experiences the most positive moment and the continuous girder for live load (c) experiences the least with a 14% difference between the two. Dead loads are supported by simply supported girders in all cases since girder self-weight and deck dead loads are present before the retrofit making the bridge continuous for live load.

Therefore, the primary advantage of eliminating the expansion joints with simply supported girders is not for strength purposes, but to simplify design and construction, and to eliminate issues resulting from water, deicing salts, and other debris passing through the expansion joint onto the supporting substructure. Making the deck slab continuous is a much simpler design strategy to reduce the number of expansion joints for new structures.

For existing bridge structures, although using the UHPC link may not produce large capacity gains, smaller gains may significantly extend the life of the bridge by marginally improving capacity and rating factors and reducing maintenance efforts at the expansion joints. A current example of the effort to reduce maintenance costs at expansion joints using UHPC is the Wilmington Viaduct Bridge Rehabilitation Project (Nizamoff 2023).

When constructing BNs and determining RFs for the example bridge made continuous for live load, the dead loads are assumed to be supported by the simply supported spans, and the live load effects are determined assuming a continuous two-span structure.

4.7 Structural Bayesian Networks

When using a BN to model structural reliability, the limit state function, $g(R, Q)$, is a natural extension of the network allowing direct determination of the structural probability of failure. The component capacity is calculated using the geometric values and material properties with their associated bias and COV values. Similarly, the live and dead load effects are provided directly as input variables with assumed bias and coefficient of variation (COV) values accounting for variable uncertainty. The nominal values used in the example BNs, in addition to their statistical attributes, are provided in Table 4.1. Using all of these provided values, the BN model can then estimate discretized distributions for the load effects, and also the component capacities. All BN development

and evaluation were performed using Netica (Norsys 2019).

4.7.1 Moment Networks

Roberts et al. 2019, Groeneveld et al. 2021, and Roberts et al. 2023 describe the methodology used in this study where structural reliability is modeled using a BN. The example BN shown in Fig. 4.1 represents the network used for a prestressed girder. For the flexural model (using the design as shown in Figs. 4.2-4.3 and assuming rectangular beam behavior), the nominal moment capacity AASHTO 2020 is determined using:

$$\begin{aligned} M_n &= f_{ps} A_{ps} \left(d - \frac{a}{2} \right) \\ &= f_{ps} A_{ps} \left(h - \frac{\sum_{i=1}^{4} A_i y_i}{A_{ps}} - \frac{a}{2} \right) \end{aligned} \tag{4.2}$$

$$a = 0.85 \left(\frac{A_{ps} f_{pu}}{0.7225 f_c' b_{eff} + k A_{ps} f_{pu} / d} \right) \tag{4.3}$$

$$f_{ps} = f_{pu} \left(1 - k \frac{c}{d} \right) \tag{4.4}$$

$$k = 2 \left(1.04 - \frac{f_{py}}{f_{pu}} \right) \tag{4.5}$$

where f_{ps} is the average stress in prestressing steel, f_c' is the compressive strength of the concrete, A_{ps} is the total area of prestressing steel, $A_i y_i$ provides the area and vertical location of prestressing strands for the i^{th} layer, $d = h - (\sum_{i=1}^{4} A_i y_i)/A_{ps}$ represents the distance from the extreme compression fiber to the prestressing steel centroid with h being the height of the girder, a represents the depth of the equivalent compression block, f_{pu} is the tensile strength of the prestressing steel, $f_{py} = 0.85 f_{pu}$ is the yield strength of the prestressing steel, b_{eff} is the effective flange width of the girder, and k is the tendon value. Rectangular beam behavior is considered a valid approximation since

the depth of the equivalent compression block is within the deck when three standard deviations of the block depth are considered.

This representation of the girder moment capacity uses the $\sum_{i=1}^{4} A_i y_i / A_{ps}$ calculation to include one additional intermediate node (As_yprod) to provide the sum of the products $\sum_{i=1}^{4} A_i y_i$. It can be shown that if the distributions for the area (A_i) and elevations (y_i) are assumed to be normal, then the sum of the products can be estimated as a normal distribution Groeneveld et al. 2021, Seijas-Macías and Oliveira 2012 under certain conditions. The primary advantage of this approach is to reduce the size of the required conditional probability tables (CPTs).

Most of the remaining BN nodes are constructed assuming normal distributions and using the nominal, bias, and COV values provided in Table 4.1. Mean values are estimated using the bias (μ = bias$\cdot$nominal), and standard deviations are calculated using the COV (σ = COV $\cdot\, \mu$). The prestressing steel area, concrete compressive strength, and live and dead load effect nodes are all constructed assuming normal distributions, and discretized into 20 bins with a total width of eight standard deviations ($\mu \pm 4\sigma$). The higher number of bins is needed to have a relatively fine approximation for the normal distribution.

The final node in the BN is the limit state node. The limit state function is defined as $g(R, Q) = R - Q$, with R and Q being the capacity and load, respectively. The limit state node uses this relationship and simply subtracts the total load effect distribution from the moment capacity distribution.

4.8 Material Deterioration

A bridge structure, through a lifetime of use, can experience decreased capacity caused by actual structural damage or deterioration. Structural damage can range from

Table 4.1: Parameters of variables used in bayesian networks of four-girder example bridge

Definition of variables	Notation	Nominal value	Bias $\left(\frac{\mu}{nominal}\right)$	COV $\left(\frac{\sigma}{\mu}\right)$	References[a] for bias/cov
Concrete compressive strength	f'_c	20.68 MPa (3.0 ksi)	1.10	0.18	LE08
Strand tensile strength[b]	f_{pu}	1861.58 MPa (270.0 ksi)	1.04	0.02	LE08
Total strand area[c]	A_{ps}	3,356.12 mm^2 (5.202 in^2)	-	-	
Top layer	A_4	197.42 mm^2 (0.306 in^2)	1.011	0.013	LE08
Top middle layer	A_3	789.68 mm^2 (1.224 in^2)	1.011	0.013	LE08
Bottom middle layer	A_2	1,184.51 mm^2 (1.836 in^2)	1.011	0.013	LE08
Bottom layer	A_1	1,184.51 mm^2 (1.836 in^2)	1.011	0.013	LE08
Centroid total strand steel[d]	$y_{c.g.}$	From layer distributions	-	-	
Top layer	y_4	203.2 mm (8.0 in)	1.00	SD[e]	NYT94
Top middle layer	y_3	152.4 mm (6.0 in)	1.00	SD[e]	NYT94
Bottom middle layer	y_2	101.6 mm (4.0 in)	1.00	SD[e]	NTY94
Bottom layer	y_1	50.8 mm (2.0 in)	1.00	SD[e]	NYT94
Simply Supported - Live Load[f]	$M_{Q_{LL}}$	2,008.64 kN·m	1.40	0.18	NS00 &
		(17,778.0 kip·in)	-	-	NC12
Simply Supported - Dead Load[g]	$M_{Q_{DL}}$	2,225.24 kN·m	1.05	0.10	NO95
		(19,695.0 kip·in)	-	-	-
Continuous - Live Load[f]	$M_{Q_{LL}}$	1,590.01 kN·m	1.40	0.18	NS00 &
		(14,072.81 kip·in)	-	-	NC12
Continuous - Dead Load[g]	$M_{Q_{DL}}$	2,225.24 kN·m	1.05	0.10	NO95
		(19,695.0 kip·in)	-	-	-
Effective flange width[h]	b_{eff}	3,048.0 mm (120 in)	-	-	-
Girder height[h,i]	h	1,587.5 mm (62.5 in)	-	-	-

[a] LE08:LeBeau 2008; NYT94:Nowak et al. 1994; NS00:Nowak and Szerszen 2000; NC12:Nowak and Collins 2012; NO95:Nowak 1995. [b] Stress relieved strands with 12.7 mm (0.5 in) diameter.
[c] Total strand area is a normal distribution resulting from the sum of normal distributions for each individual strand. The bias and COV are used for each strand. At the center of the girder, the top, top middle, bottom middle, and bottom layers have 2, 8, 12, and 12 strands, respectively. The girder has 34 total strands.
[d] Vertical distances to strand centroids are referenced to bottom girder edge. [e] The error in positioning layer reinforcement does not change based on the depth of the member. Therefore, the variability of the vertical positioning, y_i, of the prestressing strands is given in terms of the standard deviation rather than COV. A standard deviation of $\sigma_{C.G.}$=17.78 mm (0.7 in) is used for each layer. [f] Live load includes an impact factor of 1.33 and distribution factor of 0.74 for an interior girder. [g] Dead load is the same for both simple/continuous cases since simply supported girders support DL in all cases. [h] Effective width and height of the girder are considered deterministic. [i] Girder height includes 215.9 mm (8.5 in) for deck thickness.

impacts to overloading caused by large trucks. Although there are many causes, common deterioration modes for concrete include corrosion of reinforcement, freeze/thaw (FT) cycling, and the alkali-silica reaction (ASR). The BNs being considered will only include specific defects caused by these deterioration modes as shown in Table 4.2. A detailed description of these deterioration modes can be found in Groeneveld et al. 2021. BNs can also be used to include information gained using existing non-destructive evaluation (NDE) methods. Determination of structural component deterioration, location of reinforcement, and determining dimensions of structural components are examples of how NDE can be used ACI 2013, Bertola et al. 2022. Additionally, basic material properties, such as concrete compressive strength can be found by sampling sections of existing structures, or using in-place techniques ACI 2019.

Table 4.2: Common defects correlated with deterioration modes

Defect	Deterioration mode
Cracking	Corrosion, FT Effect, ASR
Spalling	Corrosion, FT Effect, ASR
Delamination	Corrosion, FT Effect
Efflorescence	FT Effect, ASR
Rust staining	Corrosion
Exposed reinforcement	Corrosion
Pattern cracking	ASR

The defects described above, and listed as Table 4.2, are presented as nodes in the BNs so that findings can be reported to the network. For example, inspection findings are shown in Fig. 4.6 at a condition state CS1 level. The severity of each defect is defined consistent with the MBEI AASHTO 2013, which means the defects range from CS1 (good) to CS4 (severe). All of the nodes have choices available from CS1 to CS4, except for pattern cracking which has a yes/no choice consistent with the presence/absence of the defect. Using the provided defects, the network provides a reduced concrete compressive

strength shown as the *Reduced* f_c' node. More discussion about the reduction of concrete compressive strength is provided in Groeneveld et al. 2021 and Roberts et al. 2023.

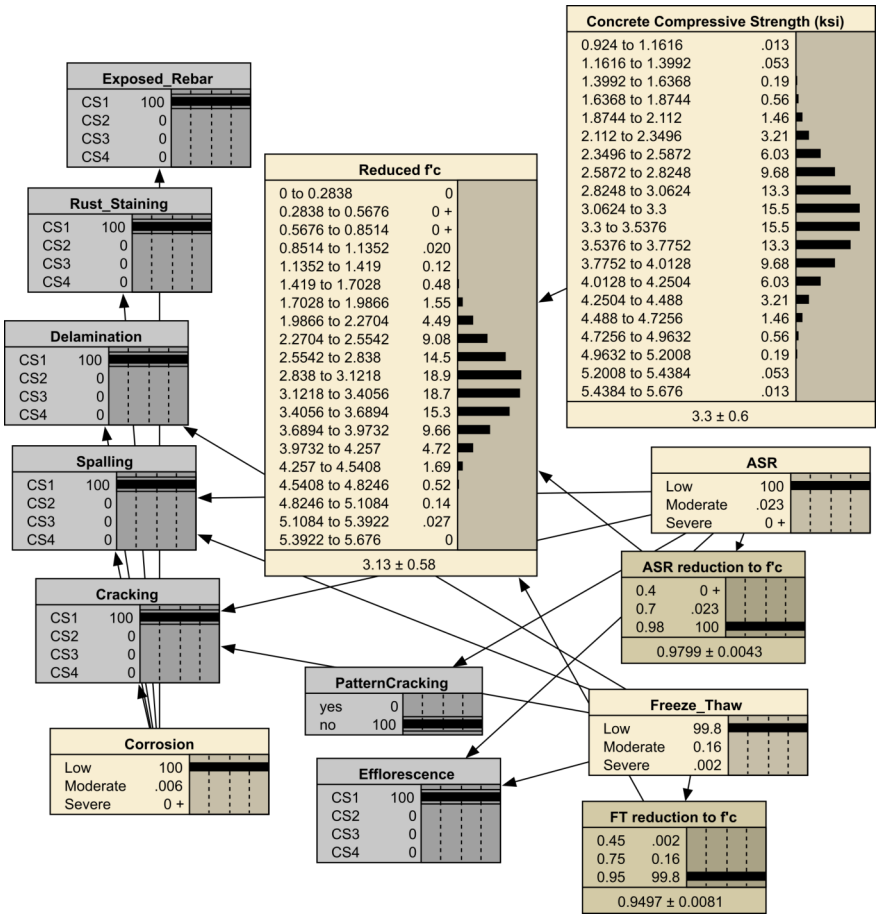

Figure 4.6: Example BN with defects assumed at condition state CS1. Defects include: exposed reinforcement, rust staining, delamination, spalling, cracking, pattern cracking, and efflorescence. Initial concrete compressive strength has mean and standard deviation of 22.75 MPa (3.3 ksi) and 4.14 MPa (0.60 ksi), respectively. The *Reduced* f_c' node provides final concrete compressive strength after CS1 defect findings are entered, and has mean and standard deviation of 21.58 MPa (3.13 ksi) and 4.00 MPa (0.58 ksi), respectively.

Conditional probability tables (CPTs) were constructed to link the considered defects shown in Table 4.2 to deterioration modes. The CPTs, resulting from expert elicitation, are used as an estimate of the relative impact of defects on concrete compressive strength. More information regarding the development and use of the CPTs can be found in

Groeneveld et al. 2021 and Roberts et al. 2023.

4.9 Bayesian Networks of Example Bridge

As previously described, the example bridge was originally constructed with both spans being connected using link blocks as shown in Fig. 4.4. During bridge inspections, deterioration and cracking of the link blocks were identified. Because of this, the bridge is considered to be structurally simply supported. Two BNs were constructed. The first was made using the assumption that the two spans act independently and are incapable of transferring internal forces between spans. The second BN was constructed assuming that the continuity joint was sufficiently repaired and the original design intent of a continuous span for live load was restored. Both BNs used the same girder positive moment capacity. However, the continuous span was exposed to a reduced positive moment load effect because of the indeterminate nature of the continuous span. In both cases, trucks were marched across the spans to determine the governing load effects AASHTO 2020.

4.9.1 BN with Spans Continuous for Live Load

With the spans acting as if they are continuous, the structure will have a increased RF for positive moment near midspan when compared to a simply supported span. This is because the positive moment load effect will be decreased for a continuous span. As previously described, when using conventional methods AASHTO 2014, AASHTO 2011 to determine the RF, the tension stress limit state governs and the following values were found for the flexure limit state: $RF_{inv} = 1.68$ and $RF_{oper} = 2.14$. For simplicity, only flexure limit states are being illustrated in this example using BNs.

The first BN was constructed to represent the moment capacity and loading of the

continuous prestressed girder, shown in Fig. 4.7. The live load node, MQ_LL is scaled using RF = 1.67. This BN represents the conditions that result in a $P_f = 2.196 \times 10^{-4}$ which provides a reliability index of $\beta_{P_f} = -\Phi^{-1}(2.196 \times 10^{-4}) = 3.52$. The reliability index can also be determined directly from the definition: $\beta_{calc} = \mu_g/\sigma_g = 3.58$. Since normal distributions are being used in the BN, the values for the reliability indexes are expected to be very similar, regardless of which method is used. If a scaling factor of RF = 1.95 is used, then $P_f = 6.420 \times 10^{-3}$ resulting in $\beta_{P_f} = -\Phi^{-1}(6.420 \times 10^{-3}) = 2.49$ and $\beta_{calc} = \mu_g/\sigma_g = 2.46$. These scaling factors are the inventory and operating rating factors: $RF_{cont\_inv} = 1.67$ and $RF_{cont\_oper} = 1.95$. Rating factor results are included in Table 4.3.

Table 4.3: Girder moment rating factor results. LRFR results use $\phi_C = 1.0$ to represent lack of defects resulting in no capacity reduction. BN results use CS1 defects to represent minor defects with slight capacity reduction. Target reliability indexes for inventory and operating rating factors are 3.5 and 2.5, respectively. To approach target reliabilities, modified LRFR factors (ϕ_{conc}, γ_{LL}) are provided.

Method	Resistance	Inventory		Operating	
	ϕ_{conc}	RF	$(\gamma_{LL}, \gamma_{DL})$	RF	$(\gamma_{LL}, \gamma_{DL})$
Current LRFR - simple	1.0	1.68	(1.75, 1.25)	2.14	(1.35, 1.25)
BN - simple	-	1.37	-	1.58	-
Current LRFR - continuous LL	1.0	2.10	(1.75, 1.25)	2.72	(1.35, 1.25)
BN - continuous LL	-	1.67	-	1.95	-
Modified LRFR - simple	0.9	1.34	(1.85, 1.25)	1.55	(1.60, 1.25)
Modified LRFR - simple	0.85	1.30	(1.75, 1.25)	1.51	(1.50, 1.25)
Modified LRFR - continuous LL	0.9	1.69	(1.85, 1.25)	1.95	(1.60, 1.25)
Modified LRFR - continuous LL	0.85	1.64	(1.75, 1.25)	1.91	(1.50, 1.25)

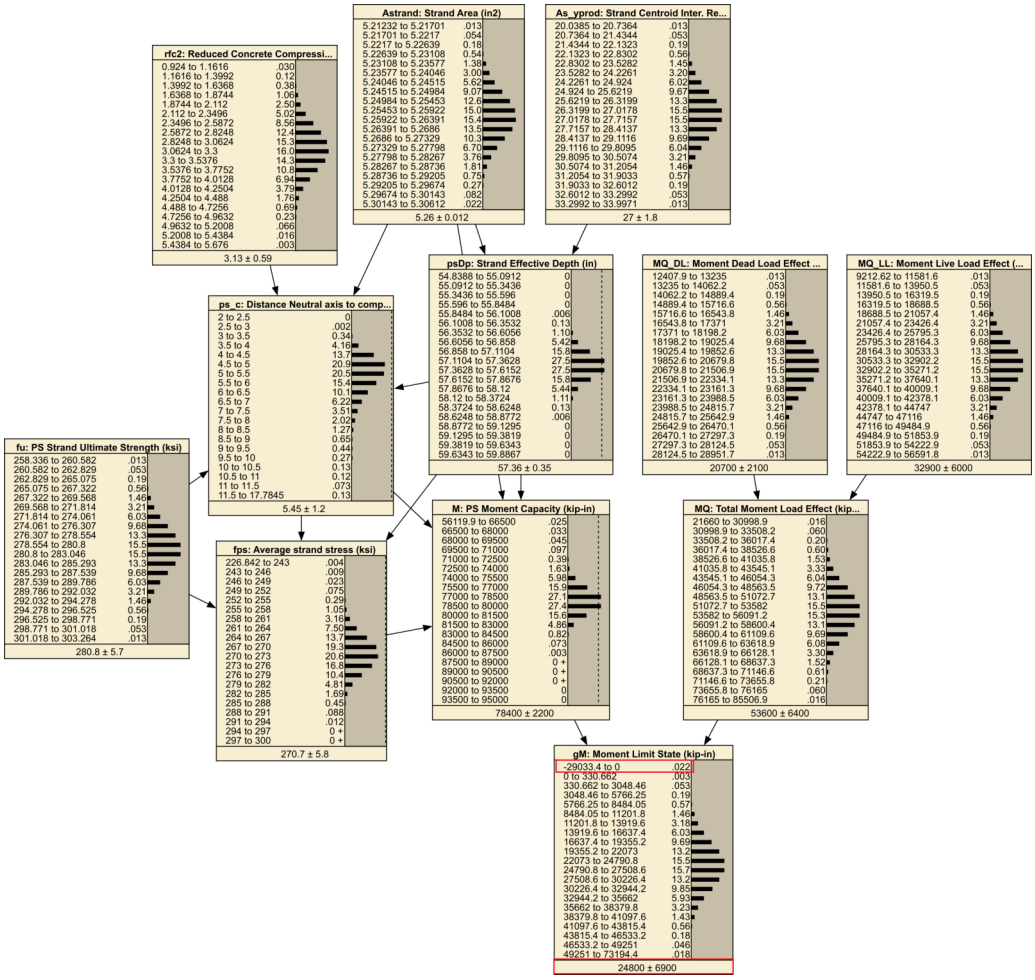

Figure 4.7: PC girder moment BN with discretized distributions for bridge continuous for live load. Live load node (MQ_LL) scaled using RF=1.67. Area of moment limit state function where $g(R,Q) < 0$ provides probability of failure, $P_f = 2.196 \times 10^{-4}$. Moment limit state mean and standard deviation are μ_g = 2,802.02 kN·m (24,800 kip·in) and σ_g = 779.60 kN·m (6,900 kip·in), respectively. $\beta_{calc} = \mu_g/\sigma_g = 3.58$. $\beta_{P_f} = -\Phi^{-1}(2.196 \times 10^{-4}) = 3.52$.

4.9.2 BN with Simply Supported Spans

With the spans acting as if they are simply supported, the structure will have a reduced RF for positive moment at span midspan, when compared to a continuous span. This is because the positive moment load effect will be increased for a simple span. As previously described, when using conventional methods AASHTO 2014, AASHTO 2011

to determine the RF, the following values were found: $RF_{inv} = 1.68$ and $RF_{oper} = 2.14$.

The second BN was constructed to represent the moment capacity and loading of the simply supported prestressed girder. An image showing this BN is not included, but would be very similar to that shown in Fig. 4.7 for a continuous span. The live load node, MQ_LL was scaled with two values to result in reliability indexes of 3.5 and 2.5, to represent the inventory and operating conditions: $RF_{simple\_inv} = 1.37$ and $RF_{simple\_oper} = 1.58$. Rating factor results are included in Table 4.3.

4.10 Conclusions

A primary advantage of using a BN to model the loading and capacity of structures is that the P_f is a direct result from the network. If a link has been developed between defects found during inspections and reduced component capacity, then an updated P_f can be determined, leading to an updated reliability index. Very easily the user can have a sense of the magnitude of loss of structural reliability. An asset manager can then use these values to determine priorities when allocating time and funding for maintenance efforts and, when necessary, structural replacement.

Bridge asset managers use load ratings to measure the ability of a bridge to support a specific live load. The current LRFR AASHTO 2018 methodology is related to LRFD AASHTO 2020 techniques, but has an added nuance in the form of the system factor, ϕ_S, and condition factor, ϕ_C. These factors are used to reduce the component capacity, when required, to account for lack of redundancy, and defects that are detected during the bridge inspection process. The condition factor is tied to the rating determined by the bridge inspection, and is a rudimentary method to account for defects. For example, the MBE AASHTO 2018 states that a component rated *Poor* should be assigned a condition factor of 0.85, *Fair* should be assigned a value of $\phi_C = 0.95$, and *Good* or *Satisfactory*

would be assigned a value of $\phi_C = 1.0$. As previously mentioned, the product $\phi_C \phi_S$ is not allowed to have a value less then 0.85. This requires the factored capacity, ϕM_n, to be reduced by 15%, due to the condition factor only, with no additional analysis required.

A more direct, and rational, approach would be to use BNs to determine the P_f, reliability index, and rating factors for bridge components. However, the examples provided illustrate differences when comparing rating factors when using BNs and the conventional methods provided by AASHTO. Note that all cases being considered assumed that the defect level is such that no reduction of moment capacity is assumed when calculating the RF using conventional methods.

As shown in Table 4.3, the rating factors for the simply supported condition vary, where the BN provides lower values for both inventory (1.37 vs. 1.68) and operating (1.58 vs. 2.14) rating factors. Additionally, the rating factors for the continuous span vary also, where the BN provides lower values for both inventory (1.67 vs. 2.10) and operating (1.95 vs. 2.72) rating factors. These differences may be due to the approximation techniques and assumptions used when determining the LRFD/LRFR load and resistance factors. Modified LRFD/LRFR factors that produce RFs found using BNs are provided in Table 4.3. The conclusion from these comparisons is necessarily limited since multiple variables may impact results, such as length of span. The example bridge has a span of around 23.8 meters (78 ft). Results from a parametric analysis may show that longer spans, in addition to other attributes, will have differing results regarding reliability and rating factors. An additional extension of the current research is to extend the concrete deterioration model to include the reduction of cross-sectional area of prestressing strands due to corrosion.

4.11 Data Availability Statement

Some or all data, models, or code that support the findings of this study are available from the corresponding author upon reasonable request. Applicable items are Netica BN models.

4.12 Acknowledgments

The authors thank the U.S. Army Corps of Engineers for the use of as-built data for bridges in the current inventory. Additionally, support from the U.S. Army and Corps (through participation in ERDC-University and funding of Projects 476923 & 154349) is acknowledged.

Edgardo Ruiz was formerly at the U.S. Army Engineer Research and Development Center, Vicksburg, MS, at the time of this research and is now affiliated with Fickett Structural Solutions, Inc.

4.13 References

American Association of State Highway Officials (AASHTO) (2011). *Manual for Bridge Evaluation*. AASHTO, Washington, D.C., 2nd edition.

American Association of State Highway Officials (AASHTO) (2013). *Manual for Bridge Element Inspection*. AASHTO, Washington, D.C., 1st edition. 2015 interims.

American Association of State Highway Officials (AASHTO) (2014). *LRFD Bridge Design Specifications*. AASHTO, Washington, D.C., 7th edition.

American Association of State Highway Officials (AASHTO) (2017). *LRFD Bridge Design Specifications*. AASHTO, Washington, D.C., 8th edition.

American Association of State Highway Officials (AASHTO) (2018). *Manual for Bridge Evaluation*. AASHTO, Washington, D.C., 3rd edition.

American Association of State Highway Officials (AASHTO) (2020). *LRFD Bridge Design Specifications*. AASHTO, Washington, D.C., 9th edition.

American Concrete Institute (ACI) (2013). *Report on Nondestructive Test Methods for Evaluation of Concrete in Structures - 228.2R*. ACI, Farmington Hills, MI.

American Concrete Institute (ACI) (2019). *Report on Methods for Estimating In-Place Concrete Strength - 228.1R*. ACI, Farmington Hills, MI.

Bertola, N., Henriques, G., Schumacher, T., and Brühwiler, E. (2022). "Engineering of existing structures: The need and place for non-destructive evaluation." *International Symposium on Nondestructive Testing in Civil Engineering*, Zurich, Switzerland. (August 16-18, 2022).

Campbell, L., Snyder, L., Whitehead, J., Connor, R., and Lloyd, J. (2019). "Probability of detection study for visual inspection of steel bridges: Volume 2 - full project report." *Joint Transportation Research Program Publication FHWA/IN/JTRP-2019/22*, Indiana Dept. of Transportation.

Casey, C. (2019). "Ultra-high performance concrete for connections of precast, prestressed girders made continuous for live load." M.S. thesis, University of Oklahoma, Norman, OK.

Federal Highway Administration (FHWA) (2022). *National Bridge Inventory*. LTBP InfoBridge: Analytics, Washington, D.C., <https://infobridge.fhwa.dot.gov/BarStackChart> (Feb. 19, 2023).

Freyermuth, C. (1969). "Design of continuous highway bridges with precast, prestressed concrete girders." *PCI Journal*, 14(2), 14–39 (https://doi.org/10.15554/pcij.04011969.14.39).

Groeneveld, A., Wood, S., Ruiz, E., and Roberts, J. (2021). "Estimating bridge reliability by using bayesian networks." *U.S. Army Corps of Engineers Engineer (USACE) Research and Development Center (ERDC)*.

LeBeau, K. (2008). "A bi-directional load rating model of the flexural response of a prestressed concrete bridge beam element." Ph.D. thesis, Northeastern University, Boston, MA.

Looney, T., Volz, J., and Floyd, R. (2021). "Behavior of a 3-span continuous bridge before and after continuity joint replacement using ultra-high-performance concrete." *Journal of Performance of Constructed Facilities*, 35(6), 04021087 (http://dx.doi.org/10.1061/(ASCE)CF.1943-5509.0001667).

Moore, M., Pares, B., Graybeal, B., Rolander, D., Washer, G., and Wiss, J. (2001). "Reliability of visual inspection for highway bridges volume 1." *Report No. FHWA-RD-01-105*, Turner-Fairbank Highway Research Center.

Nizamoff, D. (2023). "UHPC link slabs and the wilmington viaduct bridge rehabilitation project." *International Interactive Symposium on Ultra-High Performance Concrete*, 3(1) (https://doi.org/10.21838/uhpc.16666).

Norsys (2019). *Netica 6.07*. Norsys Software Corp, Vancouver, Canada.

Nowak, A. (1995). "Calibration of LRFD bridge code." *Journal of Structural Engineering*, 121(8), 1245–1251.

Nowak, A. and Collins, K. (2012). *Reliability of Structures*. CRC Press.

Nowak, A. and Szerszen, M. (2000). "Structural reliability as applied to highway bridges." *Progress in Structural Engineering and Materials*, 2(2), 218–284.

Nowak, A., Yamani, A., and Tabsh, S. (1994). "Probabilistic models for resistance of concrete bridge girders." *American Concrete Institute Structural Journal*, 91(3), 269–276.

Roberts, J., Ruiz, E., Groeneveld, A., and Pérez-Gracia, R. (2019). "Use of bayesian networks for inferences on bridge safety." *Proceedings of the 98th Annual Meeting of the Transportation Research Board*, Washington, DC. (Jan 13-17, 2019). Presentation no. 19-04278.

Roberts, J., Schumacher, T., Groeneveld, A., Wood, S., and Ruiz, E. (2023). "Estimating reinforced concrete bridge reliability with inspection defects included using bayesian networks." *Manuscript submitted for publication*.

Seijas-Macías, A. and Oliveira, A. (2012). “An approach to distributions of the product of two normal variables.” *Discussiones Mathematicae Probability and Statistics*, 87–99 (http://dx.doi.org/10.7151/dmps.1146).

Texas Department of Transportation (TxDOT) (2001). *Bridge Design Manual*. TxDOT, Austin, TX.

5 Chapter Five: Summary and Future Work

5.1 Summary

The purpose of this research was to develop a methodology for modeling existing bridge structures so that estimates of the probability of failure, P_f, and by extension a measure of reliability, β, could be determined. This results in an improved ability to objectively determine which structures should be maintained or replaced. This is particularly useful when budgets are limited and maintenance and replacement priorities can be objectively determined. BNs were developed for both flexure and shear limit states illustrating the idea that BNs can be developed using simple structural mechanics.

BN models were developed and presented for several bridges using three primary material types: reinforced concrete, prestressed (pretensioned) concrete, and steel. Since all relevant information for determining bridge load ratings are present within the BN, rating factors were also determined for all considered bridges by scaling live loads to achieve specific target reliability indexes.

The LRFR rating process uses resistance factors to account for condition and lack of redundancy in the structural system. Combined, these two factors are allowed to reduce member capacity by as much as 15%. The current work shows how BNs can be used to directly account for material deterioration modes. The required conditional probability tables (CPTs) required to link modes and defects found during inspections can be considered the current state of the art and can be updated as more expertise is gained. This decreases the impact of a key subjective component of the inspection process. Additionally, using system reliability to account for series and parallel systems of individual components, a P_f estimate can be determined for individual components, bridge spans, or an entire bridge.

There are various methods of performing a sensitivity analysis, but a fully formed BN can also provide guidance to which elements of a structure has the most impact on structural reliability. But, the overall benefit of this system of using BNs to represent a bridge (or other structural systems) is to have an ongoing tally of the reliability of the structure as the structure ages. This is a rational approach linking capacity, deterioration modes, detectable defects, and the required decisions related to whether the structure is fulfilling it's intended purpose.

5.2 Future Work

Possible avenues for future work include the following:

- The current work uses expert elicitation to link several deterioration modes and varying levels of defect severity. Additional research and testing would be appropriate to strengthen and better understand this link and to include additional deterioration modes leading to more confidence in the CPTs. This could include lab tests of specially fabricated specimens and also field tests of existing structures, using both destructive and NDT methods.

- Extend the concrete models to include the influence of corrosion on bond properties between concrete and reinforcement. Although the decrease in bond is expected to have more impact, the reduction of cross-sectional area of reinforcing steel due to corrosion should also be included. Current BN models account for specific deterioration modes by reducing the compressive strength of concrete. Including loss of bond and steel area reduction would extend the ability of the BNs to more completely model flexural and shear capacity.

- The current BNs depend on the nominal values of design parameters, such as

structure dimensions and steel and concrete properties. Using the potential of the BN approach includes using actual statistical values of these properties, including both in-service structures and structures scheduled for demolition. For in-service structures, NDT methods could be used to determine the statistical distributions of element dimensions (e.g. width, depth) and actual locations of reinforcement. As previously mentioned, the modulus of elasticity and compressive strength can also be determined using cores or NDT techniques. Regarding old structures that are slated for demolition, all of these techniques can be used to develop in-kind information of similar structures that are still in-service.

- Extend the structural steel model to include section loss through corrosion. This would be applicable to bridges using both rolled steel and built-up sections.

- To develop the P_f of a system (e.g., multiple segmented girders with various defects plus deck), a range of P_f values was developed, leading to a range of reliability indexes for the system. The P_f lower bound applies when the failures of the components are completely dependent and the Pf upper bound applies when the failures are considered completely independent. For simplicity and to be conservative, the highest P_f (and lowest reliability index) was chosen. However, a better understanding of how to model the independent vs. dependent nature of the structural components would be beneficial.

- All of the BNs used a discretized distribution to model material properties. When these properties are used to define a child node, the new distributions can become skewed. A method to manage the child discretized distributions would be necessary in order to minimize artificial skewing and automate the creation and use of BNs.

- An extension of this research would be to couple an existing open source load

rating software package with the use of BNs. An example of this is software named PGSuper from the Washington State DOT which is used specifically for prestressed girders and is a fully capable example of bridge load rating and design software. Similarly, the current research uses proprietary software to model BNs. An alternative would be to develop BNs in R or Python allowing a fully open source solution to using BNs to load rate bridges using prestressed girders.

- The current research focused on relatively simple bridge structures with the longitudinal girder being the primary member. Extending the research to more complicated structures would be a logical, but not trivial, next step. The Corps designs, builds, and maintains water gates of various types. Examples of these include miter gates used as part of the locking chamber used to pass vessels past a dam structure. Being able to model these types of structures would be advantageous from an asset management point of view. Since these types of gates have 3-D behavior, effort would be needed to simplify the more complicated behavior to 1-D or 2-D approximations. An alternative would be combining finite element software directly with the BN software.

- Understand data and methods used to develop current LRFD/LRFR load and resistance factors to explain differences between reliability indexes and RFs found using LRFR and BNs.

- Each node of a BN is impacted by other nodes in the network. Knowledge of the sensitivity to a change in the mean and standard deviation of other nodes can have a practical use to the user of a BN so that certain structural elements can be favored. For example, if the yield strength of reinforcement is found to impact the reliability of the structure (i.e. the P_f is sensitive to f_y), then effort would be justified to better understand the statistical parameters of that node. Better understanding the

sensitivity of nodes used in the structural BNs would give direction to further testing of component material properties.